

The strength of the interaction between quarks and gluons

(ALPHA collaboration)

Mattia Dalla Brida^{1,2}, Roman Höllwieser³, Francesco Knechtli³,
Tomasz Korzec³, Alberto Ramos⁴, Stefan Sint⁵, Rainer Sommer^{6,7}

¹Dipartimento di Fisica, Università di Milano-Bicocca, Piazza della
Scienza 3, I-20126 Milano, Italy.

²INFN Milano-Bicocca, Piazza della Scienza 3, Milan, I-20126, Italy.

³Department of Physics, Bergische Universität Wuppertal, Gaußstr. 20,
42119 Wuppertal, Germany.

⁴Instituto de Física Corpuscular (IFIC), CSIC-Universitat de Valencia,
46071, Valencia, Spain.

⁵School of Mathematics and Hamilton Mathematics Institute, Trinity
College Dublin, Dublin 2, Ireland.

⁶John von Neumann Institute for Computing (NIC), DESY,
Platanenallee 6, 15738 Zeuthen, Germany.

⁷Institut für Physik, Humboldt-Universität zu Berlin, Newtonstr. 15,
12489 Berlin, Germany.

Abstract

Modern particle physics experiments, e.g. at the Large Hadron Collider (LHC) at CERN, crucially depend on the precise description of the scattering processes in terms of the known fundamental forces. This is limited by our current understanding of the strong nuclear force, as quantified by the strong coupling, α_s , between quarks and gluons. Relating α_s to experiments poses a major challenge as the strong interactions lead to the confinement of quarks and gluons inside hadronic bound states. At high energies, however, the strong interactions become weaker (“asymptotic freedom”) and thus amenable to an expansion in powers of the coupling. Attempts to relate both regimes usually rely on modeling of the bound state problem in one way or another. Using large scale numerical simulations of a first principles formulation of Quantum Chromodynamics on a space-time lattice, we have carried out a model-independent determination of α_s

with unprecedented precision. The uncertainty, about half that of all other results combined, originates predominantly from the statistical Monte Carlo evaluation and has a clear probabilistic interpretation. The result for α_s describes a variety of physical phenomena over a wide range of energy scales. If used as input information, it will enable significantly improved analyses of many high energy experiments, by removing an important source of theoretical uncertainty. This will increase the likelihood to uncover small effects of yet unknown physics, and enable stringent precision tests of the Standard Model. In summary, this result boosts the discovery potential of the LHC and future colliders, and the methods developed in this work pave the way for even higher precision in the future.

Keywords: QCD, Perturbation Theory, Lattice QCD

PAC Codes: 12.38.Aw , 12.38.Bx , 12.38.Gc , 11.10.Hi , 11.10.Jj

Properties of the strong interactions

At the fundamental level, the strong nuclear force between nucleons arises from Quantum Chromo Dynamics (QCD), a quantum field theory formulated in terms of their “colour-charged” elementary constituents, the quarks and gluons. The strength of the quark-gluon coupling, $\alpha_x(\mu)$, depends on the energy scale, μ , of the interaction and also on its detailed definition, summarized as “scheme”, x .

Quarks do not appear as free particles but are confined in colour-neutral hadronic states such as protons, neutrons or π -mesons. Quark confinement arises due to $\alpha_x(\mu)$ becoming large at typical hadronic energy scales below a GeV, where μ approaches Λ_x , the characteristic scale or Λ -parameter of QCD. The absence of free quarks makes it impossible to measure the coupling directly in experiment.

The scale dependence of the strong coupling is described by its β -function,

$$\mu \frac{d}{d\mu} \alpha_x(\mu) = \beta_x(\alpha_x(\mu)). \quad (1)$$

which has an expansion of the form $\beta_x(\alpha_x) = -\beta_0 \alpha_x^2 - \beta_1 \alpha_x^3 + O(\alpha_x^4)$, with leading *positive* coefficients β_0, β_1 which are independent of the scheme. This implies that $\alpha_x(\mu)$ “runs” with the scale μ , decreasing for increasing μ , with a leading behaviour $\propto 1/\ln(\mu/\Lambda_x)$ as shown in figure 1. This phenomenon, known as asymptotic freedom [1, 2] implies that perturbative series expansions in powers of the strong coupling become accurate at high energies, as exemplified by the β -function itself. The scheme independence of the leading coefficients, β_0, β_1 , implies that the asymptotic scale dependence is universal and Λ -parameters of different schemes are simply related by exactly calculable constants.

Conventionally, $\Lambda_{\text{QCD}} \equiv \Lambda_{\overline{\text{MS}}}$ is used for a reference, where $\overline{\text{MS}}$ stands for the modified minimal subtraction scheme [3]. Knowledge of Λ_{QCD} and the β -function is equivalent to knowing the coupling at any given scale μ . In the $\overline{\text{MS}}$ scheme, the

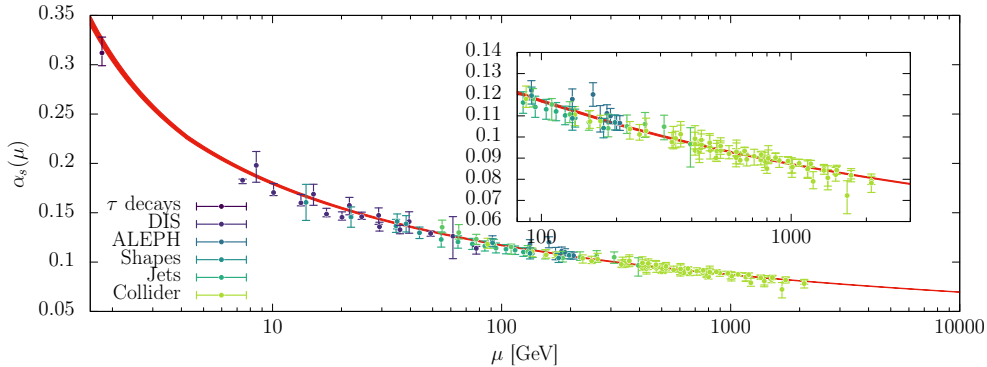


Fig. 1: The strong coupling for a wide range of energy scales, as determined from our result for Λ_{QCD} , is represented by the red band. Also shown are experimental determinations from various processes with their uncertainties as quoted by the Particle Data Group (PDG) [9].

expansion coefficients of $\beta_{\overline{\text{MS}}}$ are known to high order including β_4 , i.e. 5-loop order [4–8], so that the scale dependence of $\alpha_{\overline{\text{MS}}}(\mu)$ can be accurately predicted down to μ of order 1 GeV. In this paper we determine Λ_{QCD} using large scale simulations.

With decades of theoretical and experimental efforts to parameterize the effects of confinement, and to identify observables where these effects are minimized, the theoretically expected scale dependence could be verified from experiments as illustrated by the data points in figure 1. However, the uncertainties due to the required modelling of confinement are hard to quantify and this often means that increased statistics is of limited use.

The rôle of lattice QCD

The modelling of confinement is entirely by-passed in lattice QCD, a genuinely non-perturbative formulation of QCD on a (Euclidean) space-time lattice with spacing a . Quark and gluon fields are sampled on the lattice points and edges, respectively. If the space-time volume is finite, the number of QCD degrees of freedom is reduced to a finite albeit large number, enabling the numerical evaluation of observables by large scale computer “simulations”. Predictions for hadronic observables, such as the proton’s mass m_p or the leptonic decay width of π -mesons, can be obtained for a given choice of the Lagrangian parameters, the bare quark masses and bare coupling, with the latter controlling the lattice spacing. In order to make contact with the natural world, one needs to take the continuum limit, $a \rightarrow 0$, based on numerical data for a range of a -values, finite volume effects must be controlled, and the bare quark masses must be tuned in order to match the physical values of the chosen experimental input.

In a volume large enough to accommodate hadrons, the typical momentum cutoff π/a is in the range 6 – 15 GeV. This is one order of magnitude below the universal large energy region, where low order perturbation theory is accurate. Together with the basic requirement that physical scales have to be well below the cutoff, $\mu \ll \pi/a$,

a large volume approach to determine the strong coupling would require lattices with significantly more than 100 million lattice points (the current state of the art), along with orders of magnitude more computational resources than those presently available. Consequently we use a scheme for the running coupling where the energy scale is given by the size of the simulated world, $\mu = 1/L$. Small volumes probe the high energy regime of QCD, while large volumes probe low energy scales. The energy dependence of the coupling is obtained by simulating pairs of lattices with extents L/a and $2L/a$, and a subsequent continuum extrapolation [10]. This relates the values of the coupling separated by a factor 2 in scale. Iterating this step scaling n times, a scale change of 2^n is achieved. For QCD with $N_f = 3$ flavours the method was developed and applied [11–14] over many years. Here we reach a further significant increase in precision and the important confirmation that the continuum limit is approached smoothly. Furthermore we complement this direct approach with the “decoupling technique” of refs. [15, 16] with essential improvements, as explained below.

Scale setting using $\sqrt{t_0}$

Results from lattice simulations come in units of the lattice spacing a , e.g. $\hat{m}_p = am_p$. In order to express them in physical (energy) units, the units of the lattice spacing a must be established through an experimental input, e.g. $a = \hat{m}_p/m_p^{\text{exp}}$. To minimize the uncertainty from the conversion between lattice and physical units, we introduce an intermediate step, by first relating the experimental input to a technical (length-) scale, $\sqrt{t_0}$, derived from the gradient flow (GF) [17]. Together with colleagues in the CLS consortium, we obtained [18, 19] $\sqrt{t_0} = 0.1443(7)(13)$ fm from the leptonic decay rates of π and K mesons. Nominally more precise values are available from the literature, which differ by the choice of experimental input or discretisation of QCD, and some results include the heavier charm quark in the simulations [20–26]. We will use $\sqrt{t_0} = 0.1434(18)$ fm, which includes a rather generous uncertainty of 1.3% that covers all precise results entering the FLAG average [27], while still producing only a subdominant source of uncertainty when propagated into our result for Λ_{QCD} .

Our main computation is further split as

$$\Lambda_{\text{QCD}}\sqrt{t_0} = \mu_{\text{dec}}\sqrt{t_0} \times \frac{\Lambda_{\text{QCD}}}{\mu_{\text{dec}}}, \quad (2)$$

where $\mu_{\text{dec}} \approx 800$ MeV denotes the decoupling scale of Refs. [15, 16]. Both dimensionless factors can be computed with high precision, however, the second factor presents a major challenge and dominates the error budget. Therefore, we computed it using two methods with very different systematics: the direct approach in $N_f = 3$ and the decoupling method.

Direct approach in $N_f = 3$ QCD

We implemented the step-scaling method using two different renormalization schemes for the coupling at low and high energy scales, respectively. In the region from hadronic $\mu \approx 200$ MeV to intermediate scales $\mu \approx 4$ GeV, our finite volume scheme is based

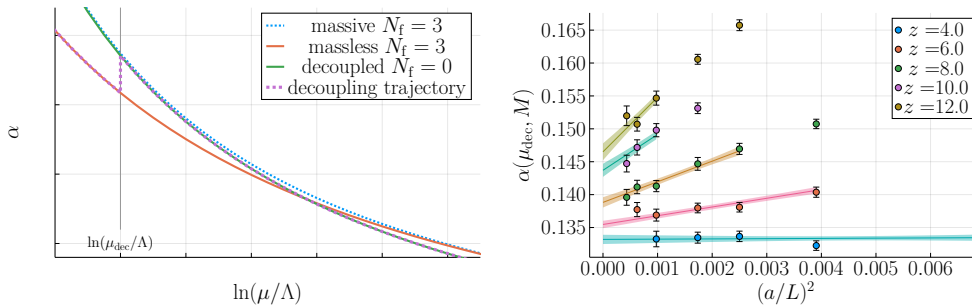


Fig. 2: Left: Illustration of the decoupling of three heavy quarks with large mass as described in the model of section 3.8. For energies $\mu \ll M$ the massive coupling runs like the pure gauge coupling, while for $\mu \gg M$ the coupling runs like the massless three flavor coupling. **Right:** Continuum extrapolation of the massive coupling $\alpha(\mu, M)$ for $z = M/\mu_{\text{dec}} = 4, 6, 8, 10, 12$. Even with the conservative cutoff in the data, $(aM)^2 < 0.16$, the extrapolated continuum values are still very precise.

on the gradient flow [11, 17] and is closely related to the low energy scale $\sqrt{t_0}$. Altogether our dataset includes 98 simulations at 10 different volumes L in the range $1/L \approx 0.2 - 4$ GeV. Compared to [12, 16] our new analysis includes a very fine lattice spacing, with $a/L = 1/64$. This allows us to improve the precision and perform crucial checks on the previous continuum extrapolation. We implicitly define an energy scale, μ_{dec} , by prescribing the value $\alpha_{\text{GF}}(\mu_{\text{dec}}) = 3.949/(4\pi)$. We then determine $\mu_{\text{dec}}\sqrt{t_0} = 1.647(17)$ which implies $\mu_{\text{dec}} = 802(13)$ MeV. For energies above μ_{dec} , we combine these results with our previous simulations of the high-energy regime in the SF scheme [14]. These include more than 40 simulations at 8 values of the volume L , that allow to explore energy scales $1/L \approx 4 - 140$ GeV non-perturbatively. An extensive analysis of the continuum limit together with a detailed exploration of the asymptotic high energy regime [28] leads to $\Lambda_{\text{QCD}}/\mu_{\text{dec}} = 0.432(11)$, which translates to our final result for the direct method, $\Lambda_{\text{QCD}} = 347(11)$ MeV. Even though a further error reduction, especially in the high energy part, appears feasible, we decided to develop an alternative: the decoupling method. It is computationally more efficient and, even more importantly, affected by very different systematics, thereby providing a strong cross-check.

The decoupling method

The idea is based on the following observation [15]. If one increases the masses of the quarks in a Gedanken-experiment, eventually the low-lying spectrum of QCD matches the spectrum of the pure gauge theory, where quarks are absent; we say they are decoupled. In this way, QCD is connected with the pure gauge theory, the theory without any quarks. Since the latter is easy to simulate, better precision can be achieved compared with QCD [29]. The exact connection requires the fundamental scale of the pure gauge theory, $\Lambda^{(0)}$ to be adjusted appropriately, $\Lambda_{\overline{\text{MS}}}^{(0)} = P(M/\Lambda_{\overline{\text{MS}}}^{(3)})\Lambda_{\overline{\text{MS}}}^{(3)}$, where in $\Lambda_{\overline{\text{MS}}}^{(N_f)}$ the number of quarks, N_f , is indicated. The matching factor P is known perturbatively to

four loop order [30] and is routinely being used to relate $\Lambda_{\overline{\text{MS}}}^{(3)} \rightarrow \Lambda_{\overline{\text{MS}}}^{(4)} \rightarrow \Lambda_{\overline{\text{MS}}}^{(5)}$, across the charm and bottom quark thresholds [31].

Decoupling works up to $\mathcal{O}(1/M^2)$ corrections, where M denotes the RGI quark mass (see methods). Detailed studies have shown [30] that the corrections are small already at masses of the order of the charm quark mass ($M_c \approx 1.4$ GeV). Here we use masses in the range $M \sim 3 - 10$ GeV, allowing us to explore the approach $M \rightarrow \infty$ in detail and safely match QCD with the pure gauge theory. Again we work in the GF scheme but in QCD with three degenerate heavy quarks.

To illustrate the procedure, the running of this massive coupling $\alpha_{\text{GF}}(\mu, M)$ is shown schematically in figure 2 (left). For energies well below their mass, the heavy quarks are decoupled and α_{GF} runs like in pure gauge theory (green line) while at μ far above their mass the running is governed by the massless β -function; it is slowed down.

We now follow the magenta trajectory in the figure. Below μ_{dec} we reuse the running in the mass-less theory. Then, at fixed $\mu = \mu_{\text{dec}}$, we increase the mass of all three quarks artificially to very high values, eventually to $M \approx 10$ GeV, following the vertical part of the magenta trajectory. At the resulting value of the massive coupling, we switch to the pure gauge theory and run to large μ where $\Lambda_{\text{GF}}^{(0)}$ is obtained. Converted (exactly) to the $\overline{\text{MS}}$ scheme, we then use the accurate high order relation $P(M/\Lambda_{\overline{\text{MS}}}^{(3)})$ between the Λ -parameters with and without quarks to revert to $\Lambda_{\overline{\text{MS}}}^{(3)} = \Lambda_{\text{QCD}}$.

The main challenge is the continuum extrapolation of the massive coupling from our simulation results at finite a . On the one hand the quark mass has to be large for the decoupling approximation to be as accurate as possible. On the other hand the mass has to be below the momentum cutoff $\sim \pi/a$ of the lattice. In other words we need $aM \ll 1$ and a good understanding of the asymptotic behavior of discretisation effects close to the continuum limit. To this end, we determined an improved discretisation such that linear effects in the lattice spacing are absent. With the result of [32] we could cancel the dangerous terms proportional to aM . Next, sufficiently small lattice spacings were simulated and we performed a combined extrapolation of the results for different quark masses and different lattice spacings. Analyzing the theory for discretization effects [33] in an expansion in $1/M$, one arrives at an asymptotic form of the discretization errors with only two free parameters. This form fits the data, figure 2, remarkably well. The fit tells us that the coupling changes from $\alpha_{\text{GF}}(\mu, M) = 0.4184(22)$ for $M \approx 3$ GeV to $\alpha_{\text{GF}}(\mu, M) = 0.4600(41)$ for $M \approx 10$ GeV in continuum QCD.

We then matched to the pure gauge theory by equating $\alpha(\mu; M)$ with the $N_f = 0$ coupling. Using previous results in the pure gauge theory from [29], we arrive at an estimate of $\Lambda_{\text{QCD}}/\mu_{\text{dec}}$ at each value of the quark mass. These estimates should all agree up to the mentioned $\mathcal{O}(1/M^2)$ corrections. Indeed the numbers are very close: for quark masses between 5 to 10 GeV, $\Lambda_{\text{QCD}}/\mu_{\text{dec}}$ varies by 5%. They also follow the expected $c_0 + c_1 M^{-2}$ behavior. An extrapolation with this form thus yields our final number $\Lambda_{\text{QCD}}/\mu_{\text{dec}} = 0.4264(97)$ in the three flavor theory from the decoupling strategy. Together with the value for μ_{dec} , we get $\Lambda_{\text{QCD}} = 341.9(9.6)$ MeV. The uncertainty covers the statistical errors and several variations of the functional form

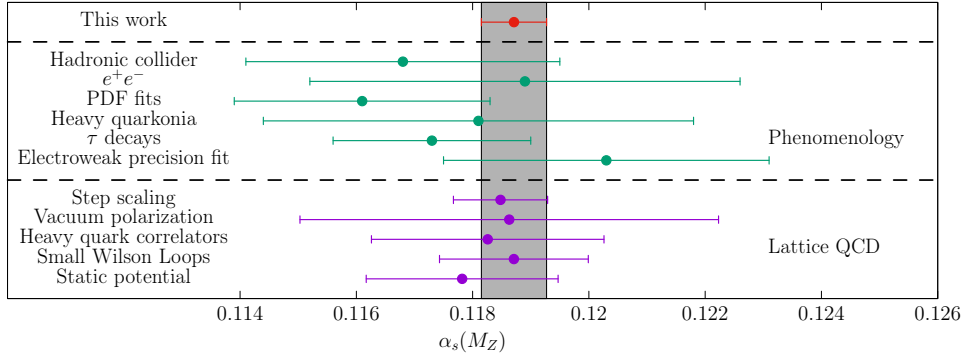


Fig. 3: Our result for $\alpha_s(m_Z)$ compared with other results from the literature (cf. text).

employed in the continuum, $a \rightarrow 0$, and decoupling, $M \rightarrow \infty$, extrapolations. It also includes the uncertainty of the conversion from $\Lambda_{\overline{\text{MS}}}$ of the pure gauge theory to Λ_{QCD} .

Final result and concluding remarks

Both the above methods to extract Λ have uncertainties dominated by statistics. Theoretical uncertainties, in particular those related to the use of perturbation theory are subdominant. The systematics are also very different in both methods, and their agreement further corroborates the robustness of our methodology. An average is justified and leads to

$$\Lambda_{\text{QCD}} = 343.9(8.4) \text{ MeV}. \quad (3)$$

We then include the charm and bottom contributions in the running in the $\overline{\text{MS}}$ scheme in perturbation theory and arrive at the curve in figure 1. In particular we have,

$$\alpha_s(m_Z) = 0.11873(56), \quad (4)$$

where $\alpha_s = \alpha_{\overline{\text{MS}}}^{(N_f=5)}$. Figure 3 shows our result compared with numbers from other strategies. Most of them have uncertainties dominated by theoretical or systematic effects, as quoted by the PDG for the phenomenology results and by FLAG for lattice results [34]. An exception is the category labeled “Step Scaling”, that uses the methods developed along the years by the ALPHA collaboration. This result is dominated by our earlier computation [14].

What have we learned? Recall that QCD is a complicated non-linear theory with the observed particles completely different from the fundamental quanta in the Lagrangian. Still, surprisingly, we are able to determine the intrinsic scale Λ_{QCD} of the theory and equivalently the coupling between quarks and gluons. A conceptual achievement beyond the mere precision of α_s is that it is determined with experimental low energy input from the decays and masses of hadrons which are all bound states of quarks and gluons. Fig. 1 compares the resulting coupling with phenomenological determinations. While the latter have their issues, the overall qualitative agreement

confirms QCD as the single theory of the strong interactions at all energies both small and large compared to Λ_{QCD} . Thus there is very little room for any modifications/additions to the theory of the strong interactions. The size of the error band demonstrates that our value can be used to better understand the physics involved in these processes, and to boost the discovery potential of the LHC. For example, our sub-percent precision in α_s is needed to control predictions such as Higgs production through gluon-fusion at the high luminosity LHC [35] and as a constraint in the determination of the hadronic Parton Distribution Functions (PDFs) [9, 36].

References

- [1] Gross, D. J. & Wilczek, F. Ultraviolet Behavior of Nonabelian Gauge Theories. *Phys. Rev. Lett.* **30**, 1343–1346 (1973).
- [2] Politzer, H. D. Reliable Perturbative Results for Strong Interactions? *Phys. Rev. Lett.* **30**, 1346–1349 (1973).
- [3] Bardeen, W. A., Buras, A. J., Duke, D. W. & Muta, T. Deep Inelastic Scattering Beyond the Leading Order in Asymptotically Free Gauge Theories. *Phys. Rev. D* **18**, 3998 (1978).
- [4] van Ritbergen, T., Vermaseren, J. A. M. & Larin, S. A. The Four loop beta function in quantum chromodynamics. *Phys. Lett.* **B400**, 379–384 (1997).
- [5] Czakon, M. The Four-loop QCD beta-function and anomalous dimensions. *Nucl. Phys.* **B710**, 485–498 (2005).
- [6] Baikov, P. A., Chetyrkin, K. G. & Kühn, J. H. Five-Loop Running of the QCD coupling constant. *Phys. Rev. Lett.* **118**, 082002 (2017).
- [7] Luthe, T., Maier, A., Marquard, P. & Schröder, Y. Towards the five-loop Beta function for a general gauge group. *JHEP* **07**, 127 (2016).
- [8] Herzog, F., Ruijl, B., Ueda, T., Vermaseren, J. A. M. & Vogt, A. The five-loop beta function of Yang-Mills theory with fermions. *JHEP* **02**, 090 (2017).
- [9] Navas, S. *et al.* Review of particle physics. *Phys. Rev. D* **110**, 030001 (2024).
- [10] Lüscher, M., Weisz, P. & Wolff, U. A Numerical method to compute the running coupling in asymptotically free theories. *Nucl.Phys.* **B359**, 221–243 (1991).
- [11] Fritzsche, P. & Ramos, A. The gradient flow coupling in the Schrödinger Functional. *JHEP* **1310**, 008 (2013).
- [12] Dalla Brida, M. *et al.* Determination of the QCD Λ -parameter and the accuracy of perturbation theory at high energies. *Phys. Rev. Lett.* **117**, 182001 (2016).

- [13] Dalla Brida, M. *et al.* Slow running of the Gradient Flow coupling from 200 MeV to 4 GeV in $N_f = 3$ QCD. *Phys. Rev.* **D95**, 014507 (2017).
- [14] Bruno, M. *et al.* QCD Coupling from a Nonperturbative Determination of the Three-Flavor Λ Parameter. *Phys. Rev. Lett.* **119**, 102001 (2017).
- [15] Dalla Brida, M. *et al.* Non-perturbative renormalization by decoupling. *Phys. Lett. B* **807**, 135571 (2020).
- [16] Dalla Brida, M. *et al.* Determination of $\alpha_s(m_Z)$ by the non-perturbative decoupling method. *Eur. Phys. J. C* **82**, 1092 (2022).
- [17] Lüscher, M. Properties and uses of the Wilson flow in lattice QCD. *JHEP* **08**, 071 (2010). [Erratum: *JHEP* 03, 092 (2014)].
- [18] Bruno, M., Korzec, T. & Schaefer, S. Setting the scale for the CLS 2 + 1 flavor ensembles. *Phys. Rev. D* **95**, 074504 (2017).
- [19] Strassberger, B. *et al.* Scale setting for CLS 2+1 simulations. *PoS LATTICE2021*, 135 (2022).
- [20] [ETM 21] C. Alexandrou *et al.* Ratio of kaon and pion leptonic decay constants with $N_f = 2 + 1 + 1$ Wilson-clover twisted-mass fermions. *Phys. Rev. D* **104**, 074520 (2021).
- [21] [CalLat 20A] N. Miller *et al.* Scale setting the Möbius domain wall fermion on gradient-flowed HISQ action using the omega baryon mass and the gradient-flow scales t_0 and w_0 . *Phys. Rev. D* **103**, 054511 (2021).
- [22] [MILC 15] A. Bazavov *et al.* Gradient flow and scale setting on MILC HISQ ensembles. *Phys. Rev.* **D93**, 094510 (2016).
- [23] [HPQCD 13A] R. Dowdall, C. Davies, G. Lepage and C. McNeile. V_{us} from π and K decay constants in full lattice QCD with physical u , d , s and c quarks. *Phys.Rev.* **D88**, 074504 (2013).
- [24] [RQCD 22] G. S. Bali *et al.* Scale setting and the light baryon spectrum in $N_f = 2 + 1$ QCD with Wilson fermions. *JHEP* **05**, 035 (2023).
- [25] [RBC/UKQCD 14B] T. Blum *et al.* Domain wall QCD with physical quark masses. *Phys. Rev.* **D93**, 074505 (2016).
- [26] [BMW 12A] S. Borsanyi *et al.* High-precision scale setting in lattice QCD. *JHEP* **1209**, 010 (2012).
- [27] Aoki, Y. *et al.* FLAG Review 2021 (2021).

- [28] Dalla Brida, M. *et al.* A non-perturbative exploration of the high energy regime in $N_f = 3$ QCD. *Eur. Phys. J. C* **78**, 372 (2018).
- [29] Dalla Brida, M. & Ramos, A. The gradient flow coupling at high-energy and the scale of SU(3) Yang-Mills theory (2019).
- [30] Athenodorou, A. *et al.* How perturbative are heavy sea quarks? *Nucl. Phys. B* **943**, 114612 (2019).
- [31] Herren, F. & Steinhauser, M. Version 3 of RunDec and CRunDec. *Comput. Phys. Commun.* **224**, 333–345 (2018).
- [32] Dalla Brida, M. *et al.* Heavy Wilson Quarks and $O(a)$ Improvement: Nonperturbative Results for b_g (2023).
- [33] Husung, N., Marquard, P. & Sommer, R. Asymptotic behavior of cutoff effects in Yang-Mills theory and in Wilson’s lattice QCD. *Eur. Phys. J. C* **80**, 200 (2020).
- [34] Aoki, Y. *et al.* FLAG Review 2024 (2024).
- [35] Salam, G. *The strong coupling: a theoretical perspective*, Ch. Chapter 7, 101–121. URL https://www.worldscientific.com/doi/abs/10.1142/9789813238053_0007. https://www.worldscientific.com/doi/pdf/10.1142/9789813238053_0007.
- [36] Sirunyan, A. M. *et al.* Determination of the strong coupling constant $\alpha_S(m_Z)$ from measurements of inclusive W^\pm and Z boson production cross sections in proton-proton collisions at $\sqrt{s} = 7$ and 8 TeV. *JHEP* **06**, 018 (2020).

1 Methods

1.1 The scale of QCD and the Λ parameter

We consider QCD with N_f quark flavours and show how an intrinsic scale can be defined, the QCD Λ -parameter. In what follows we adopt the conventions of our past papers and use the coupling $\bar{g}_x(\mu) = \sqrt{4\pi\alpha_x(\mu)}$. The β -function, as a function of \bar{g}_x , is given by,

$$\mu \frac{\partial \bar{g}_x(\mu)}{\partial \mu} = \beta_x(\bar{g}_x), \quad (5)$$

We emphasize that β_x is non-perturbatively defined if this is the case for the coupling \bar{g}_x . As mentioned earlier, the first two coefficients in the expansion $\beta_x(g) = -b_0 g^3 - b_1 g^5 + O(g^7)$,

$$b_0 = \left(11 - \frac{2}{3}N_f\right) \times (4\pi)^{-2}, \quad b_1 = \left(102 - \frac{38}{3}N_f\right) \times (4\pi)^{-4}, \quad (6)$$

are renormalization-scheme independent (β_k of Eq. (1) is proportional to b_k , for $k = 0, 1, \dots$). This asymptotic behaviour for small couplings allows us to integrate the

differential equation (5) between the scales μ and μ' as follows,

$$\frac{\mu'}{\mu} = \exp \int_{\bar{g}_x(\mu)}^{\bar{g}_x(\mu')} \frac{dg}{\beta_x(g)} = \frac{\varphi_x(\bar{g}_x(\mu))}{\varphi_x(\bar{g}_x(\mu'))}. \quad (7)$$

Here, the function φ_x is given by,

$$\varphi_x(\bar{g}_x) = (b_0 \bar{g}_x^2)^{-b_1/(2b_0^2)} e^{-1/(2b_0 \bar{g}_x^2)} \times \exp \left\{ - \int_0^{\bar{g}_x} dg \left[\frac{1}{\beta_x(g)} + \frac{1}{b_0 g^3} - \frac{b_1}{b_0^2 g} \right] \right\}. \quad (8)$$

Note that, by design, the integrand in the exponent is regular at zero coupling. Furthermore, the combination $\mu \varphi_x(\bar{g}_x(\mu))$ is independent of μ , has units of energy and is known as the Λ -parameter of QCD,

$$\Lambda_x^{(N_f)} = \mu \varphi_x(\bar{g}_x(\mu)) = \mu' \varphi_x(\bar{g}_x(\mu')). \quad (9)$$

Since these equations are exact, the Λ -parameter can be evaluated at any scale μ , provided the integral in the exponent of φ_x can be evaluated reliably. This poses a particular challenge for lattice QCD: the experimental observables used to fix the free parameters, i.e. the quark masses and the lattice spacing, are measured at very low energies, where QCD is clearly non-perturbative. Matching to hadronic physics thus requires a hadronic low energy scale, μ_{had} . However, the integral extends to zero coupling, i.e. an infinitely large energy scale. The idea then is to split the computation into two factors,

$$\frac{\Lambda_x^{(N_f)}}{\mu_{\text{had}}} = \frac{\mu_{\text{pert}}}{\mu_{\text{had}}} \times \varphi_x(\bar{g}_x(\mu_{\text{pert}})). \quad (10)$$

where $\mu_{\text{pert}} \gg \mu_{\text{had}}$ is a large scale, in the perturbative regime of QCD. One then uses the non-perturbative step-scaling approach (s. below) to determine the large scale ratio (first factor), together with the values of the coupling at both scales. The second factor is evaluated in perturbation theory, by inserting the perturbative expansion of the β -function, which is, in the $\overline{\text{MS}}$ -scheme, known up to 5-loop order. Here we use the SF scheme [1] to define μ_{pert} through $\bar{g}_{\text{SF}}^2(\mu_{\text{pert}}) = 1.085(4)$, which yields the value

$$\frac{\Lambda_{\text{SF}}^{(3)}}{\mu_{\text{pert}}} = 0.003788(88). \quad (11)$$

While the central value can be easily calculated from Eq. (8), given the value of the coupling and the 3-loop approximation of the SF β -function, the error estimate requires a careful comparison of perturbative and non-perturbative scale evolution, where the latter is obtained from the step-scaling procedure (s. below). In physical units, the perturbative matching scale μ_{pert} is found to be approximately 70 GeV. By varying this scale in the range 4 – 128 GeV [2], we performed extensive tests of

perturbation theory and our final choice combines moderate statistical errors with significantly smaller systematic errors.

The Λ -parameter is scheme dependent. Given two mass-independent schemes x and y , with the respective couplings related perturbatively by

$$g_x^2 = g_y^2 + c_{xy}g_y^4 + \dots \quad (12)$$

we have the exact relation

$$\Lambda_x/\Lambda_y = \exp(c_{xy}/2b_0), \quad (13)$$

i.e. the scheme-dependence is completely encoded in the perturbative one-loop coefficients relating the respective couplings. This provides an indirect non-perturbative meaning for Λ -parameters defined in purely perturbative schemes like the $\overline{\text{MS}}$ -scheme, and $\Lambda_{\overline{\text{MS}}}^{(N_f)}$ is thus taken as the reference scale in QCD. For our particular case, we have $\Lambda_{\text{SF}}^{(3)}/\Lambda_{\overline{\text{MS}}}^{(3)} = 0.38286(2)$, which results in

$$\frac{\Lambda_{\overline{\text{MS}}}^{(3)}}{\mu_{\text{pert}}} = 0.00989(23). \quad (14)$$

1.2 Finite volume renormalization schemes and step scaling

In order to relate physical observables defined at very different scales by lattice simulations, the key idea is to define an intermediate renormalization scheme in a finite space-time volume, where the linear extent of the volume, L , is used to set the renormalization scale, i.e. $\mu = 1/L$. Given the renormalized coupling in such a finite volume scheme s , one then proceeds with the computation of the so called step-scaling function (SSF),

$$\sigma_x(u) = \bar{g}_x^2(\mu/2) \Big|_{\bar{g}_x^2(\mu)=u}, \quad (15)$$

which determines the coupling at scale $\mu/2$ as a function of the coupling at scale μ . The step-scaling function is closely related to the β -function,

$$\int_{\sqrt{\sigma_x(u)}}^{\sqrt{u}} \frac{dg}{\beta_x(g)} = \ln 2 \quad (16)$$

Given a finite volume coupling $\bar{g}_x(\mu)$ and its SSF $\sigma_x(u)$ for a range of u -values, one obtains the non-perturbative scale evolution of the coupling towards lower energy scales by setting $u_0 = u_{\text{min}}$ and then iterating

$$u_k = \sigma_x(u_{k-1}), \quad k = 1, 2, 3, \dots \quad (17)$$

until one exits the range of available u -values. After 10 steps one has covered a scale factor of 2^{10} , i.e. 3 orders of magnitude. Yet the non-perturbative construction of the SSF can be carried out without ever dealing with large scale differences. All that is

required are pairs of lattices of linear dimension L/a and $2L/a$, where the measured value of the coupling on the smaller lattice defines the argument u and the measured value (at the same bare parameters) on the $2L/a$ -lattice defines a lattice approximant, $\Sigma_x(u, a/L)$ to $\sigma_x(u)$. Repeating such computations for a range of lattice resolutions, a/L , then allows one to take the continuum limit

$$\sigma_x(u) = \lim_{a/L \rightarrow 0} \Sigma_x(u, a/L). \quad (18)$$

The procedure is repeated for different values u by adjusting the bare coupling g_0^2 . Note that eq. (16) can be used to obtain the β function. First one finds a suitable parametrization of the β -function. Several different choices have been made in the literature, from simple polynomials, inspired by perturbation theory [3], to Padé ansätze, suitable for a description of data at low and intermediate energy scales [4]. Once the functional form $\beta_x(x)$ is fixed, the set of parameters are determined using a standard χ^2 fit

$$\chi^2 = \sum_{i=1}^{N_{\text{pt}}} \left(\frac{\ln 2 - \int_{\sqrt{\sigma_x(u)}}^{\sqrt{u}} \frac{dg}{\beta_x(g)}}{\sqrt{[\beta(\sqrt{u})]^{-2}[\delta u]^2 + [\beta(\sqrt{\sigma_x(u)})]^{-2}[\delta \sigma_x(u)]^2}} \right)^2. \quad (19)$$

Knowledge of $\beta_x(g)$ then allows us to compute the ratio of the scales associated with two values of the coupling,

$$\ln \frac{\mu_1}{\mu_2} = \int_{\bar{g}_x(\mu_1)}^{\bar{g}_x(\mu_2)} \frac{dx}{\beta_x(x)}. \quad (20)$$

While the step-scaling strategy is straightforward in principle, its practicality depends on a number of technical details which have been developed over the last 30 years. Perturbation theory in finite volume is non-standard and can be very intricate, depending on the chosen boundary conditions. Using Schrödinger Functional (SF) boundary conditions and the standard SF coupling [1, 5], the perturbative conversion to the $\overline{\text{MS}}$ -scheme has been pushed to 2-loop order, so that the 3-loop β -function is known [6]. However, the standard SF coupling is not so well-suited at low energies, due to the increase of its variance for larger physical volumes. Schemes based on the gradient flow (GF) are much better adapted to this regime. A strategy using both couplings and a non-perturbative matching between them at an intermediate scale has been devised for QCD with $N_f = 3$ quark flavours in ref. [7]. We refer to this reference for the precise definition of the couplings in the SF and GF schemes.

These practical issues lead to a further splitting of the ratio $\mu_{\text{pert}}/\mu_{\text{had}}$ of Eq. (13) into two factors,

$$\frac{\mu_{\text{pert}}}{\mu_{\text{had}}} = \frac{\mu_0}{\mu_{\text{had}}} \times \frac{\mu_{\text{pert}}}{\mu_0}, \quad (21)$$

where μ_0 denotes the scale at which the GF and SF couplings are matched non-perturbatively. The first factor (i.e. the low energy part), is computed using the Gradient Flow scheme with Schrödinger Functional boundary conditions [8], while the second factor is computed using the SF scheme [5, 9]. This strategy combines the

advantages of both schemes: the high statistical precision of the GF scheme at low scales and the available analytic control in perturbation theory for the SF scheme.

The second factor comes from the data used in [3] together with the detailed study of the linear scaling violations and the matching with perturbation theory described in [2]. Defining μ_0 implicitly through $\bar{g}_{\text{SF}}^2(\mu_0) = 2.012$, we iterate the step scaling function 4 times, to arrive at the scale $\mu_{\text{pert}} \approx 70$ GeV, and, therefore, we have,

$$\frac{\mu_{\text{pert}}}{\mu_0} = 16. \quad (22)$$

At low energies, the simulations of [4] have been significantly improved with simulations close to the continuum limit (see table 1). Precise values in the continuum limit can be obtained for the step scaling function $\sigma(u)$, and these can be used to obtain the β -function. Defining the scales $\bar{g}_{\text{GF}}^2(\mu_{\text{had}}) = 11.31$ and $\bar{g}_{\text{GF}}^2(\mu_0/2) = 2.6723(64)$, we get the ratio,

$$\frac{\mu_0}{\mu_{\text{had}}} = 21.86(33). \quad (23)$$

so that $\mu_{\text{pert}}/\mu_{\text{had}} = 16 \times 21.86(33) = 349.8(5.3)$.

What remains to be done is the matching of μ_{had} to the experimental input. The scale μ_{had} refers to massless QCD, as the coupling is renormalized in the chiral limit. To obtain μ_{had} in MeV, we pass via the technical scale $\sqrt{t_0}$. Using an average of different works (including our own) we obtain $\sqrt{t_0} = 0.1434(18)$ fm, determined using different experimental inputs (mainly meson decay constants and hadron masses). The rather generous error of 1.3% covers all the differences, while still be sufficiently small to remain subdominant in the total error for the Λ -parameter.

Relating μ_{had} to the technical scale $\sqrt{t_0}$ is then done in two steps,

$$\mu_{\text{had}} = \frac{1}{\sqrt{t_0}} \times \sqrt{\frac{t_0}{t_0^*}} \times \left(\sqrt{t_0^*} \times \mu_{\text{had}} \right) = 200.5(3.0) \text{ MeV}, \quad (24)$$

where t_0^* is defined as the value of t_0 in QCD in the flavour symmetric limit, with Pions and Kaons of equal masses of about 410 MeV.

Here we have used [10, 11] that $\sqrt{t_0/t_0^*} = 1.0003(30)$, and, from [7], $\sqrt{t_0^*} \times \mu_{\text{had}} = 0.146(11)$.

To summarize, the step scaling procedure has allowed us to connect the scales $\mu_{\text{had}} \approx 200$ MeV with $\mu_{\text{pert}} \approx 70,000$ MeV, thereby bridging a scale factor of 350 without relying on perturbation theory.

1.3 Decoupling of heavy quarks

The basic physics principles of the decoupling strategy are summarized in the equation

$$\rho P(z/\rho) = \frac{\Lambda_{\overline{\text{MS}}}^{(0)}}{\mu_{\text{dec}}} = \frac{\Lambda_{\overline{\text{MS}}}^{(0)}}{\Lambda_{\text{GF}}^{(0)}} \times \varphi_{\text{GF}}^{(0)}(\bar{g}_{\text{GF}}(\mu_{\text{dec}}, M)). \quad (25)$$

In the following we explain the various elements one by one. First, the function P is the ratio of $\Lambda^{(0)}$ and $\Lambda^{(3)}$ in the $\overline{\text{MS}}$ scheme, where it can be extracted from the 4-loop matching of the coupling and five-loop running with very high accuracy. Its argument is the ratio $M/\Lambda_{\overline{\text{MS}}}^{(3)} = z/\rho$, where $z = M/\mu_{\text{dec}}$ involves the renormalization group invariant quark mass, M . We vary z from about 4 to 12 and for each z we extract

$$\rho = \Lambda_{\overline{\text{MS}},\text{eff}}^{(3)}(z)/\mu_{\text{dec}} = \Lambda_{\overline{\text{MS}}}^{(3)}/\mu_{\text{dec}} + \mathcal{O}(1/z^2) \quad (26)$$

as the numerical solution of equation (25). Combined with the already known μ_{dec} we obtain estimates for $\Lambda_{\overline{\text{MS}},\text{eff}}^{(3)}$. The function $\varphi_{\text{GF}}^{(0)}(g)$ is known rather precisely from the step scaling computation [12], typically with a 1% accuracy. It determines the curve labeled “decoupled” in fig. 2. The factor $\Lambda_{\overline{\text{MS}}}^{(0)}/\Lambda_{\text{GF}}^{(0)} = 0.4981(17)$ is known exactly [13], cf. eq.(13).

The values for the massive coupling, $\bar{g}(\mu_{\text{dec}}, M)$, where we evaluate $\varphi_{\text{GF}}^{(0)}$ are determined by a careful continuum extrapolation. First, as discussed before, it is crucial to remove linear effects $\sim aM$ [14]. Second, we used effective field theory (EFT) to derive the leading terms of the expansion of the lattice discretised observable, namely \bar{g}_{GF} , in a and $1/M$ in the region $aM \ll 1$ and $z \gg 1$. The EFTs are Symanzik effective theory as well as the decoupling expansion, i.e. the pure gauge theory with perturbations by dimension six operators. The latter provide corrections to the infinite M limit. These EFTs have to be applied in the correct order: the decoupling expansion is applied to the Symanzik effective theory. The crucial information obtained from the EFT analysis is that for sufficiently small $a\mu_{\text{dec}}$, aM and large z , results at finite lattice spacing are described by

$$\bar{g}_{\text{GF}}^2(\mu_{\text{dec}}, M, a) = \bar{g}_{\text{GF}}^2(\mu_{\text{dec}}, M, 0) + p_1[\alpha_s(a^{-1})]^{\hat{\Gamma}_{\text{eff}}} a^2 \mu_{\text{dec}}^2 + p_2[\alpha_s(a^{-1})]^{\hat{\Gamma}'_{\text{eff}}} (aM)^2, \quad (27)$$

The a^2 terms are accompanied by $\alpha_s^\Gamma(1/a)$ terms which vary logarithmically with the argument. However, the leading powers Γ , Γ' are small [15]. Our explicit tests with the available data show that including them or neglecting them has a minor effect and such variations of the analysis are part of our error budget.

Numerically, the form eq. (27) describes the data very well for a quite large range of $(a\mu_{\text{dec}})^2$ and all $z \geq 4$. In order to obtain our continuum results $\bar{g}_{\text{GF}}^2(\mu_{\text{dec}}, M, 0)$ we impose a cut of $(aM)^2 < 0.16$ but the curves in the figure do extend to larger values and show that the exact position of the cut is not relevant. Indeed, the numerical analysis also shows no evidence of higher powers in a or the mentioned logarithmic corrections. In summary, the continuum values are solid.

All that is left is to take the limit $z \rightarrow \infty$ of the estimates $\Lambda_{\overline{\text{MS}},\text{eff}}^{(3)}(z)/\mu_{\text{dec}}$. The extrapolation turns out to be smooth, with the data with $z \geq 8$ being compatible with the $M = \infty$ value. All data with $z \geq 4$ is well described by a linear functional form in $1/z^2$. Logarithmic corrections to this linear functional form have a very small effect in the final determination $\Lambda_{\overline{\text{MS}}}^{(3)}/\mu_{\text{dec}}$ (see figure 8).

We note that our definition of \bar{g}_{GF} takes place in a finite volume with boundaries in time (as opposed to periodic). In principle this feature allows for linear corrections

in a and $1/M$. The associated boundary terms in the EFTs are rather simple and we computed their effects. In our setup with $T = 2L$ they are well below the statistical uncertainties of $\bar{g}_{\text{GF}}^2(\mu_{\text{dec}}; M)$. Note that the uncertainty in the massive coupling contributes a small amount to the total uncertainty in α_s .

2 Extended data figures and tables

L/a	u	$\Sigma(u, a/L)$	L/a	u	$\Sigma(u, a/L)$
8	6.5485(61)	11.452(79)	16	6.549(15)	13.36(14)
8	5.8671(35)	9.250(66)	16	6.037(14)	11.34(10)
8	5.8648(65)	9.377(25)	16	5.867(14)	10.91(12)
8	5.3010(35)	7.953(44)	16	5.865(11)	10.810(69)
8	4.4848(24)	6.207(23)	16	5.301(13)	9.077(75)
8	3.8636(22)	5.070(16)	16	4.4901(77)	6.868(40)
8	3.2040(20)	3.968(11)	16	3.9475(58)	5.689(14)
8	2.7363(14)	3.2650(79)	16	3.8643(63)	5.485(22)
8	2.3898(16)	2.7722(63)	16	3.2029(52)	4.263(16)
8	2.1275(16)	2.4226(49)	16	2.7359(35)	3.485(11)
			16	2.3900(30)	2.9348(71)
			16	2.1257(25)	2.5360(66)
12	6.5446(81)	12.87(17)			
12	6.1291(56)	11.79(13)			
12	5.8730(46)	10.497(78)	20	5.857(11)	10.965(77)
12	5.8697(87)	10.485(36)	20	3.9493(63)	5.755(22)
12	5.2991(36)	8.686(49)			
12	4.4908(31)	6.785(36)			
12	3.9461(43)	5.592(11)	24	5.877(14)	11.09(11)
12	3.8666(24)	5.380(25)	24	3.9492(62)	5.770(25)
12	3.2058(17)	4.180(14)			
12	2.7380(15)	3.403(11)			
12	2.3903(11)	2.8963(87)	32	3.9490(97)	5.844(32)
12	2.1235(13)	2.5043(76)			

Table 1: Data used to determine the β -function in $N_f = 3$ QCD. The column labeled u represent the value of the coupling $\bar{g}_{\text{GF}}^2(\mu, a/L)$ at a scale $\mu = 1/L$ on a lattice of size L/a , while the columns labeled $\Sigma(u, a/L)$ represent the value of the coupling on a lattice twice as large. Data in bold represent the new computations on larger lattices that require simulations on lattices up to $L/a = 64$. This dataset allows a precise and accurate continuum extrapolation of the step scaling function (see Figure 4).

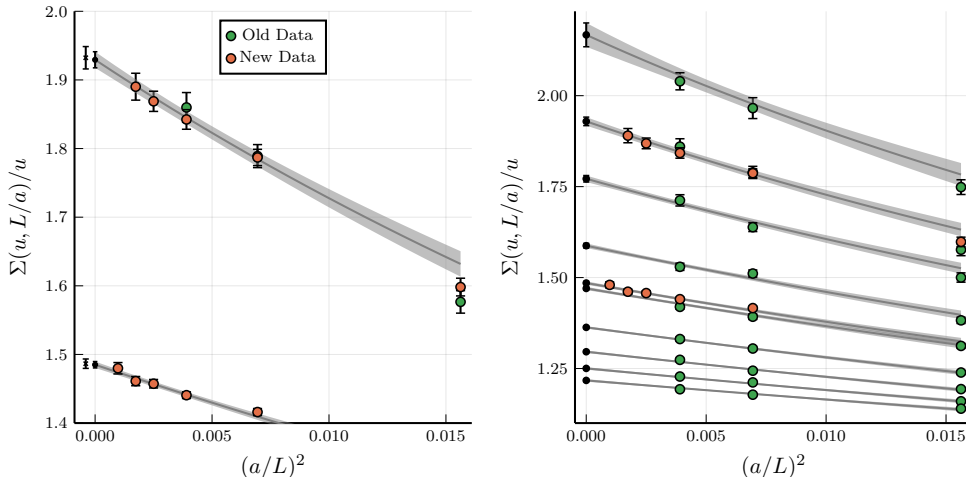


Fig. 4: Continuum limit of the step scaling function. The dataset of table 1 allows for a precise determination of the step scaling function in the continuum limit. Left: In particular at two values of the coupling ($u = 3.9490, 5.8673$) we have determined the lattice step scaling function $\Sigma(u, L/a)$ for lattice sizes up to $L/a = 32$. The continuum values are significantly improved in precision (the old continuum values are displayed with a cross), but central values have barely moved. Right: The full dataset, that includes both the new data and the old data [4].

c_M	L/a	$6/\bar{g}_0^2$	$z = M/\mu_{\text{dec}}$				
			4	6	8	10	12
-0.2	12	4.3019(16)	5.235(20)	5.614(23)	6.107(19)		
-0.2	16	4.4656(23)	5.195(29)	5.498(31)	5.892(28)		
-0.2	20	4.6018(24)	5.259(31)	5.422(29)	5.757(33)		6.481(33)
-0.2	24	4.7166(25)	5.258(33)	5.425(29)	5.678(38)	5.998(32)	6.281(30)
-0.2	32	4.9000(42)	5.255(47)	5.393(36)	5.558(33)	5.882(39)	6.065(42)
-0.2	40	5.0497(41)		5.432(42)	5.562(40)	5.792(46)	5.924(41)
-0.2	48	5.1741(54)			5.502(48)	5.699(50)	5.978(59)
-0.2	∞		5.258(28)	5.347(22)	5.479(31)	5.669(40)	5.780(51)
-0.1	∞		5.253(28)	5.346(22)	5.474(31)	5.658(39)	5.760(51)
-0.3	∞		5.262(28)	5.349(22)	5.484(31)	5.682(39)	5.799(51)

Table 2: Massive couplings at finite L/a corrected to the non-perturbative b_g value with eq. (61) and parameter $c_M = -0.2$. In the last three rows we list the continuum limits of the couplings also considering $c_M = -0.1, -0.3$. The reader can see that the effect of the parameter c_M is not significant in the values of the coupling in the continuum. The continuum limits are taken according to eq. (62) with $\Gamma_{\text{eff}} = \Gamma'_{\text{eff}} = 0$ using only the data highlighted in bold face. These satisfy the cut $(aM)^2 \leq 0.16$. Different choices of $\Gamma_{\text{eff}}, \Gamma'_{\text{eff}}$ are considered later (cf. Figure 8).

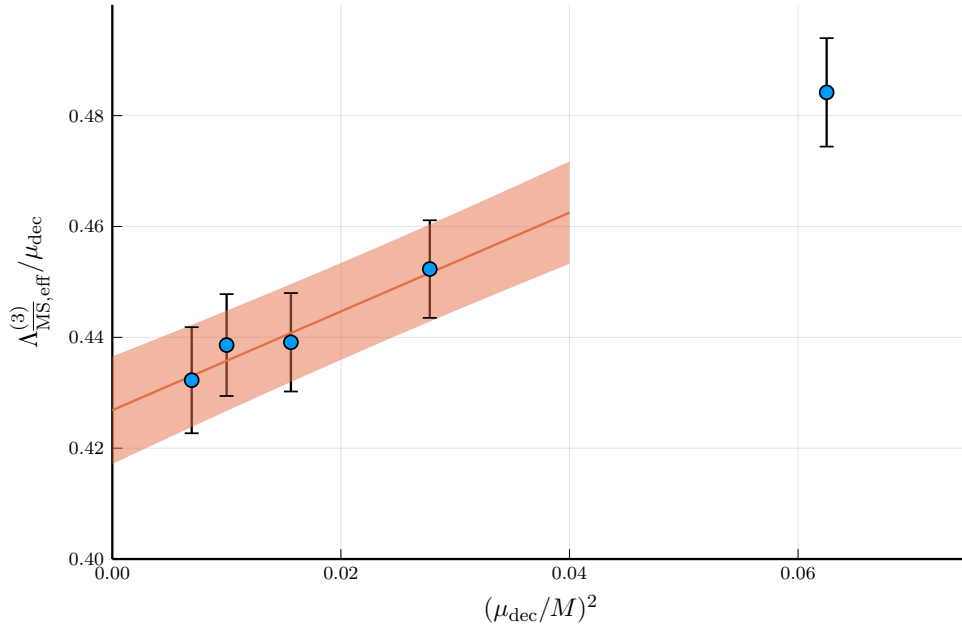


Fig. 5: In the decoupling approach the intrinsic scale of QCD is extracted after matching $N_f = 3$ QCD and the pure gauge theory using three degenerate heavy quarks of mass M . In the limit $M \rightarrow \infty$ the decoupling relation becomes exact. We performed simulations with quark masses in the range $M \approx 3 - 10$ GeV. This plot shows that the approach to infinite mass (with corrections $O(1/M^2)$) agrees with the expectations of an analysis based on effective field theory. The $M \rightarrow \infty$ limit is obtained considering only masses $M \gtrsim 5$ GeV.

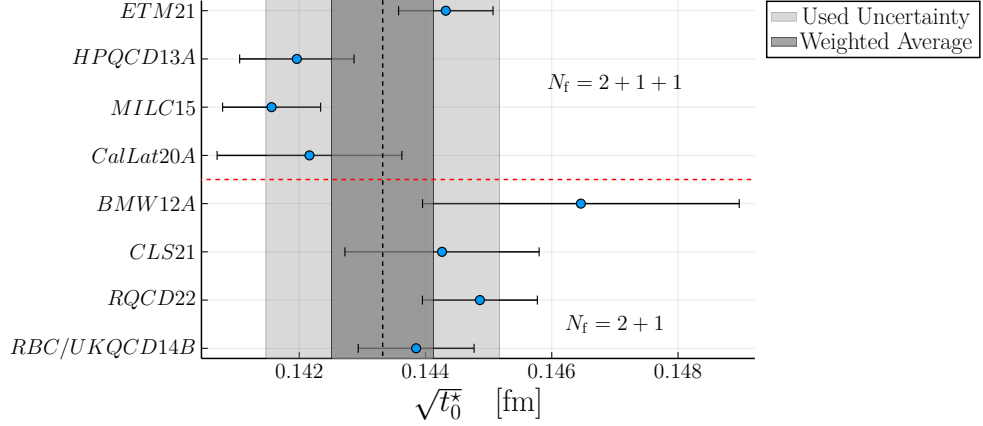


Fig. 6: The length scale $\sqrt{t_0^*}$ in fm using the ratio $\sqrt{t_0/t_0^*}$ of eq. (28) and the results for $\sqrt{t_0}$ from different collaborations [10, 11, 16–21]. Our conservative average includes the central values of all precise results, and has an uncertainty almost two times larger than a weighted average. It thus takes the presently poor agreement into account.

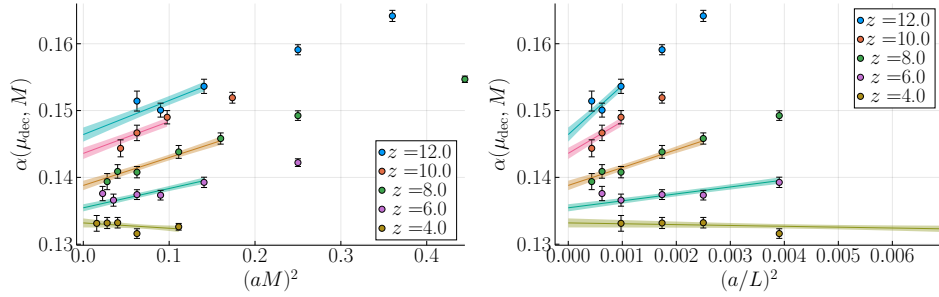


Fig. 7: Continuum extrapolation of our data for the massive coupling. Our data, after being corrected with the non-perturbative value of b_g , agrees with expectations derived from an effective field theory analysis: most cutoff effects are proportional to $(aM)^2$, with a constant slope.

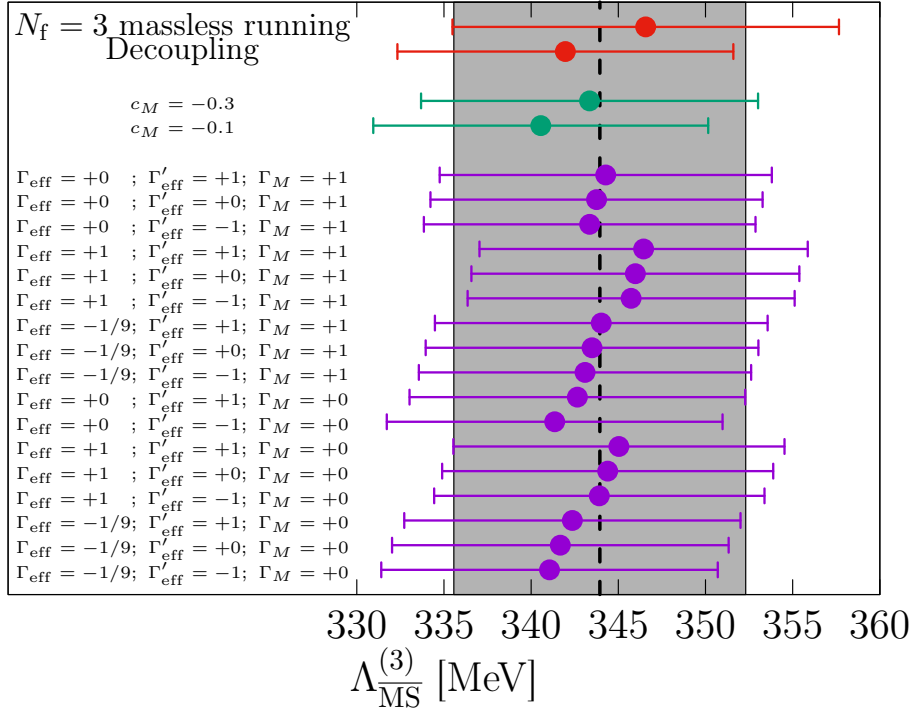


Fig. 8: The two main results, using the massless running or the decoupling strategy, are displayed in red. Our final result (a weighted average of the previous two results) is displayed by vertical the grey band. Our result for $\Lambda_{\overline{\text{MS}}}^{(3)}$ depends very little on the logarithmic corrections to the continuum extrapolation of the massive coupling Eq. (62) as well as on those in the large-mass extrapolation (75); these are all displayed by the purple points. The dependence on the linear $O(aM)$ shifts in Δb_g (green points) is even smaller (cf. the parameter c_M in Eq. (61)).

M/μ_{dec}	$\bar{g}_{\text{GFT}}^2(\mu_{\text{dec}}, M)$	$[\bar{g}_{\text{GF}}^{(0)}(\mu_{\text{dec}})]^2$	ρ^{eff}	$\Lambda_{\overline{\text{MS}}}^{\text{eff}}$ [MeV]
4	5.258(28)	4.048(18)	0.4843(98)	388.4(10.0)
6	5.347(22)	4.103(15)	0.4523(88)	362.7(9.2)
8	5.479(31)	4.184(19)	0.4390(89)	352.1(9.1)
10	5.669(40)	4.299(24)	0.4382(92)	351.4(9.3)
12	5.780(51)	4.364(31)	0.4319(96)	346.4(9.5)
M/μ_{dec}	$\hat{\Gamma}_{\text{M}}$	cut in z	ρ	$\Lambda_{\overline{\text{MS}}}$ [MeV]
∞	0	$z \geq 4$	0.4264(91)	341.7(9.2)
∞	1	$z \geq 4$	0.4323(89)	346.3(9.1)
∞	0	$z \geq 6$	0.4264(97)	341.7(9.6)
∞	1	$z \geq 6$	0.4286(95)	343.5(9.5)

Table 3: Values of the massive coupling in the continuum $\bar{g}_{\text{GFT}}^2(\mu_{\text{dec}}, M)$ and the corresponding values of the coupling in the pure gauge theory $[\bar{g}_{\text{GF}}^{(0)}(\mu_{\text{dec}})]^2$ in the $c = 0.3, T = L$ scheme. We also quote the effective Λ -parameter, both in units of μ_{dec} and in physical units. Finally we also quote the extrapolations $M \rightarrow \infty$ of the latter. The couplings themselves diverge logarithmically in this limit.

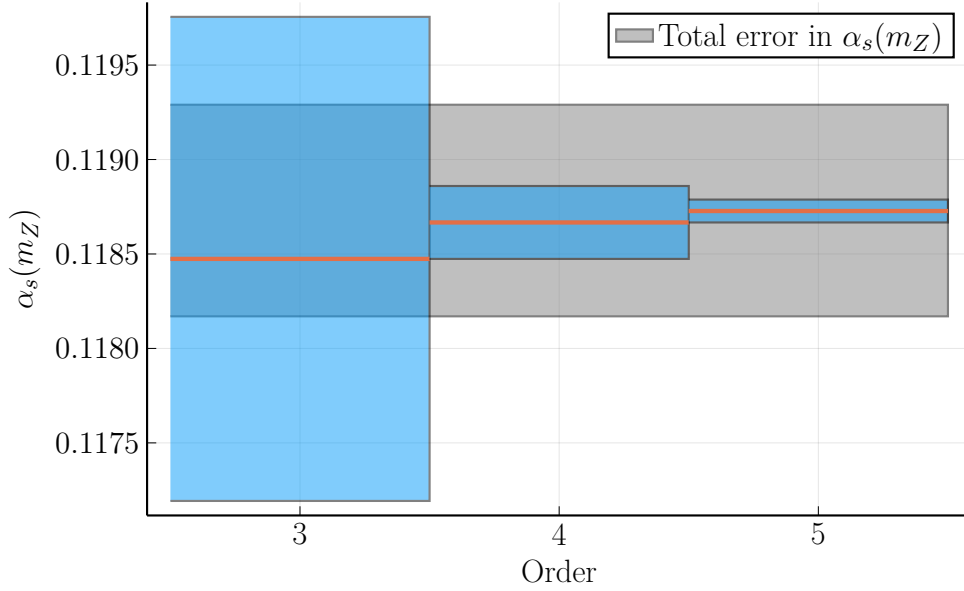


Fig. 9: Translating the value of $\Lambda_{\overline{\text{MS}}}^{(3)}$ into the value of the strong coupling requires crossing the charm and bottom quark thresholds using perturbation theory. This plot shows the perturbative uncertainties at each order $n = 3, 4, 5$. Orange horizontal lines represent $\alpha_s(m_Z)$ extracted from our central value $\Lambda_{\overline{\text{MS}}}^{(3)} = 343.9$ MeV using different orders in perturbation theory. The bands represent the perturbative uncertainties, estimated by the difference between the order n and the order $n - 1$ result. These perturbative estimates seem very conservative: for $n = 3$ and $n = 4$ the error bars are several times larger than the actual difference between the order n and the order $n + 1$. Still the perturbative uncertainty for $n = 5$ contributes less than 2% in the final error of $\alpha_s(m_Z)$.

3 Supplementary material

3.1 Scale setting

Our result for the strong coupling depends on the value of a technical scale μ_{had} that has to be determined in physical units. This scale is implicitly defined by specifying a precise value for the massless coupling in 3 flavor QCD: $\bar{g}_{\text{GF}}^2(\mu_{\text{had}}) = 11.31$ (see [7]). Ultimately, μ_{had} has to be determined from a well measured experimental quantity (like for instance the mass of the Ω baryon). In practice, it is convenient to introduce an intermediate technical length scale, $\sqrt{t_0^*}$, derived from the gradient flow [22]. This scale differs from the more common scale $\sqrt{t_0}$ by the choice of quark masses: while $\sqrt{t_0}$ is defined for physical values of the quark masses, $\sqrt{t_0^*}$ is defined for three degenerate quark masses $m_u = m_d = m_s$ such that $12t_0m_\pi^2 = 1.11$ (see [7] for further details). Our estimate for $\sqrt{t_0/t_0^*}$, is based on [10] but with an enlarged error which also covers the central value from [11]. Yet, the uncertainty on

$$\sqrt{\frac{t_0}{t_0^*}} = 1.0003(30) \quad (28)$$

is negligible for our purposes. This ratio allows us to determine $\sqrt{t_0^*}$ from the results for $\sqrt{t_0}$ from different lattice collaborations. The estimates for the reference scale $\sqrt{t_0^*}$ obtained in this way are displayed in Figure 6. We only show the computations that pass the averaging criteria set by FLAG [23].¹ These computations were performed using a range of simulations that allows for controlling the main sources of systematic uncertainties in lattice computations (i.e. continuum limit, infinite volume extrapolation, chiral extrapolation, ...). They also use different experimental quantities as input (like the mass of the Ω baryon, or leptonic decay rates of Pions and Kaons). Despite satisfying the FLAG criteria, the different data in Figure 6 show some tension. At present, there is no clear reason for this tension. Therefore we opt for a robust average. Our mean value for $\sqrt{t_0^*}$ is given by the weighted average of all results, but we increase the error to include the central values of all computations which exert a pull of two or more on the weighted average.² As a result, we use

$$\sqrt{t_0^*} = 0.1434(19) \text{ fm} . \quad (29)$$

Exploiting this result and the dimensionless combination

$$\sqrt{t_0^*} \mu_{\text{had}} = 0.1456(11) \quad [0.7\%], \quad (30)$$

that was accurately determined in [7], we can quote a value for the scale μ_{had} in physical units

$$\mu_{\text{had}} = 200.5(3.0) \text{ MeV} . \quad (31)$$

¹Note that CLS21 [11] supersedes CLS16 [7] considered in FLAG [23].

²The pull is defined as the contribution to the χ^2 of the fit to a constant. Computations with a small pull either have a central value that agrees well with the mean or they have a large uncertainty and are therefore not so relevant in determining the mean.

Despite the modest precision on this scale (1.5%), its uncertainty is subdominant in the final uncertainty of the strong coupling.

3.2 The running coupling at low energies

Once the scale μ_{had} is determined in physical units, one needs to compute the running of the coupling from $\bar{g}_{\text{GF}}^2(\mu_{\text{had}}) = 11.31$, up to high energy scales, where perturbation theory accurately describes QCD. The determination of the β function follows the strategy explained in section 1 and used in [4]. First, we determine the lattice step scaling function in the GF scheme

$$\Sigma(u, a/L) = \bar{g}_{\text{GF}}^2(\mu/2) \Big|_{\bar{g}_{\text{GF}}^2(\mu)=u}. \quad (32)$$

Our data set includes estimates of $\Sigma(u, a/L)$ from lattices with sizes $L/a = 8, 12, 16$, at nine different values of u , as considered in [4]. Moreover we have new data [24–27] much closer to the continuum, with $L/a = 20, 24, 32$, at two specific values of $u = 3.949, 5.8673$. This data set allows us to determine precisely the step scaling function in the continuum

$$\sigma(u) = \lim_{a/L \rightarrow 0} \Sigma(u, a/L). \quad (33)$$

We use a linear functional form in a^2 for the continuum extrapolations. As explained in detail in [4, 11], our data shows significant discretization effects. These are well described by a simple a^2 term, but different subleading terms, e.g., a^4 , can affect the result of the extrapolations. Therefore we opt to give less importance to the data at coarse lattice spacing. We do so by considering a weight $[\Delta_i]^{-2}$ which includes the statistical error Δ_i^{stat} and a term reducing the weight of data further away from the continuum. It has the expected dominating a^4 contamination built in,

$$\Delta_i^2 = [\Delta_i^{\text{stat}}]^2 + [\Delta_i^{\text{sys}}]^2, \quad \Delta_i^{\text{sys}} = 0.05 \Sigma_i \left(8 \frac{a}{L}\right)^4 \frac{u}{u_{\text{max}}}. \quad (34)$$

The term $[\Delta_i^{\text{sys}}]^2$ is negligible compared to our statistical uncertainties at all values of u for lattices with $L/a \geq 12$, but it becomes dominant at large values of u for $L/a = 8$. As a result, in addition to reducing the relevance of data far away from the continuum, the uncertainties of our results in the continuum are also increased. Eq. (34) is unchanged compared to our previous study [4], but we now have data closer to the continuum. A comparison of our previous extrapolations and those with the new data set show a considerable reduction of the error (cf. figure 4). Central values are in total agreement. This validates our approach to perform the continuum extrapolations.

We parameterize the β -function as

$$\beta(x) = -\frac{x^3}{P_N(x^2)}, \quad (35)$$

where $P_N(x^2)$ is a polynomial of degree N in x^2 , and extract its coefficients by fitting the continuum step scaling function data, σ , to

$$\ln 2 = \int_{\sqrt{u}}^{\sqrt{\sigma(u)}} \frac{dx}{\beta(x)}. \quad (36)$$

Alternatively one can directly fit the lattice step scaling function $\Sigma(u, a/L)$ by including the cutoff effects in the fitting ansatz as

$$\ln 2 + \left(\frac{a}{L}\right)^2 Q_{n_c}(u) = \int_{\sqrt{u}}^{\sqrt{\Sigma(u, a/L)}} \frac{dx}{\beta(x)}, \quad (37)$$

where $Q_{n_c}(u)$ is a polynomial in u of degree n_c without constant term. We obtain good fits with $N > 1$ and $n_c > 1$.³ We choose the values $N = n_c = 2$ to quote our final result for the β function, whose continuum form reads

$$\beta(x) = -\frac{x^3}{p_0 + p_1 x^2 + p_2 x^4}, \quad (38)$$

with

$$p_0 = 16.14035, \quad p_1 = 0.1817488, \quad p_2 = -0.01067877, \quad (39)$$

and covariance

$$\text{cov}(p_i, p_j) = \begin{pmatrix} +3.7345229609 \times 10^{-1} & -1.2847238140 \times 10^{-1} & +9.7506456742 \times 10^{-3} \\ -1.2847238140 \times 10^{-1} & +4.6710306855 \times 10^{-2} & -3.6595093583 \times 10^{-3} \\ +9.7506456742 \times 10^{-3} & -3.6595093583 \times 10^{-3} & +2.9433371344 \times 10^{-4} \end{pmatrix}. \quad (40)$$

This result allows us to compute some key ratios of scales. Specifically, defining

$$\bar{g}_{\text{GF}}^2(\mu_{\text{had}}) = 11.31, \quad \bar{g}_{\text{GF}}^2(\mu_{\text{dec}}) = 3.949, \quad \bar{g}_{\text{GF}}^2(\mu_0/2) = 2.6723(64), \quad (41)$$

we obtain

$$\frac{\mu_{\text{dec}}}{\mu_{\text{had}}} = 4.000(30), \quad \frac{\mu_0}{\mu_{\text{dec}}} = 5.467(62), \quad \frac{\mu_0}{\mu_{\text{had}}} = 21.86(33). \quad (42)$$

Given these ratios and the results of section 3.1, we can determine all these scales in physical units,

$$\mu_{\text{had}} = 200.5(3.0) \text{ MeV}, \quad \mu_{\text{dec}} = 802(13) \text{ MeV}, \quad \mu_0 = 4381(93) \text{ MeV}. \quad (43)$$

3.3 The strong coupling from $N_f = 3$ QCD

Given the knowledge of a hadronic scale μ_{had} determined from the QCD spectrum (see section 3.1), and a precise running of the strong coupling from $\mu_{\text{had}} \approx 200 \text{ MeV}$

³See [28] for how one determines the quality of fits with general weights such as the ones described above.

to $\mu_0 \approx 4 \text{ GeV}$ at hand, it is time to match with perturbation theory and extract the value of the strong coupling at high energy.

One may be tempted to match with perturbation theory directly at μ_0 ; in fact perturbation theory is routinely used at these energy scales. This, however, would produce a result with very small statistical uncertainties (below 0.2% in $\alpha_s(m_Z)$), but with a difficult-to-estimate theoretical uncertainty. The defining feature of the strategy pursued by the ALPHA collaboration consists instead in pushing the computation of the non-perturbative running of the coupling to much higher energies, up to the electroweak scale, where the theoretical uncertainties associated with the use of perturbation theory are negligible. The trade off is the larger statistical uncertainty that the determination of this non-perturbative running carries.

In [2, 3] we determined the ratio

$$\frac{\Lambda_{\overline{\text{MS}}}^{(3)}}{\mu_0} = 0.0791(19). \quad (44)$$

We recall that this result was obtained by matching with perturbation theory at a scale $\mu_{\text{PT}} \approx 70 \text{ GeV}$. The convergence of the perturbative approach at high energy scales was checked using three different renormalization schemes, and perturbative uncertainties were estimated in many different ways, including scale variation [2]. Our result also includes a more accurate modeling of the $\mathcal{O}(a)$ boundary effects [2]. Together with the result for μ_0 (Eq. (43)), we get

$$\Lambda_{\overline{\text{MS}}}^{(3)} = 346(11) \text{ MeV}. \quad (45)$$

Compared with our previous result [7], the central value has moved by less than half a standard deviation. This comes essentially from the change in the scale $\sqrt{t_0^*}$. Despite the fact that the new dataset reduces the uncertainty in μ_0/μ_{had} by 20%, and we also have a slight reduction of the error in $\Lambda_{\overline{\text{MS}}}^{(3)}/\mu_0$ (Eq. (44)), our determination of $\Lambda_{\overline{\text{MS}}}^{(3)}$ shows only a marginal improvement compared with our previous computation. Nevertheless, this update is important for two reasons. First, our analysis techniques, and in particular our method for calculating the continuum limit of the step scaling function at low energy, have been validated. Second, it highlights the crucial point that our uncertainties are primarily governed by the statistical uncertainties on the running in the high energy regime. In conclusion, using a non perturbative approach for computing the running of the strong coupling up to the electroweak scale, even if it removes the theoretical uncertainty, results in a substantial statistical uncertainty. This is reducible through extensive computational efforts, but would profit from an alternative strategy.

3.4 Decoupling of heavy quarks

As we commented, the uncertainty in $\Lambda_{\overline{\text{MS}}}^{(3)}$ is dominated by the high energy running. The challenge is therefore to improve the statistical uncertainty in computing the running coupling at high energies. Here we use the alternative strategy based on the

decoupling of heavy quarks introduced in [29] and applied in [30]. This approach achieves a high precision by shifting the step scaling computations from QCD to the pure gauge theory, where much better precision can be achieved (see [12, 31]).

Let us summarize the decoupling strategy as described in [30]. Using a massive scheme for the coupling, $\bar{g}_{\text{GF}}^2(\mu, M)$, where all N_f quarks are taken degenerate with renormalization group invariant (RGI) mass M , this coupling tends to its pure gauge theory counterpart in the limit of large quark masses, $M \gg \Lambda, \mu$.⁴ In formulas,

$$\bar{g}_{\text{GF}}^2(\mu, M) = [\bar{g}_{\text{GF}}^{(0)}(\mu)]^2 + \mathcal{O}(\Lambda^2/M^2, \mu^2/M^2), \quad (46)$$

where the power corrections of order Λ^2/M^2 and μ^2/M^2 were explicitly written. The shorthand notation used in this equation hides the fact that for a given μ (which we shall set equal to μ_{dec} in our numerical application), the pure gauge coupling $\bar{g}_{\text{GF}}^{(0)}(\mu)$ depends on the mass M through the matching of the Λ -parameters of the two theories, which reads,

$$\Lambda_{\overline{\text{MS}}}^{(0)} = P(\Lambda_{\overline{\text{MS}}}/M) \Lambda_{\overline{\text{MS}}}. \quad (47)$$

As discussed in [32], the function P is perturbatively known to very high accuracy. By this we mean that the relation is known to a high order in perturbation theory and the higher order corrections decrease very rapidly for the values of the masses of interest.

In perturbation theory, the function P can be computed as,

$$P(M/\Lambda_{\overline{\text{MS}}}) = \frac{\varphi_{\overline{\text{MS}}}^{(0)}(g_\star \sqrt{C(g_\star)})}{\varphi_{\overline{\text{MS}}}(g_\star)}. \quad (48)$$

In this equation $\varphi_{\overline{\text{MS}}}^{(0)}(g)$ and $\varphi_{\overline{\text{MS}}}(g)$ refer to the function (8) for 0 and 3 flavours, respectively, in the $\overline{\text{MS}}$ scheme. The coupling $g_\star = \bar{g}_{\overline{\text{MS}}}(m_\star)$, where m_\star is defined by the implicit equation $m_\star = \bar{m}_{\overline{\text{MS}}}(m_\star)$ with $\bar{m}_{\overline{\text{MS}}}(\mu)$ the running quark mass in the $\overline{\text{MS}}$ scheme at the scale μ (see section 3.6). Note that the coupling g_\star is a function of $M/\Lambda_{\overline{\text{MS}}}$ alone, i.e. $g_\star \equiv g_\star(M/\Lambda_{\overline{\text{MS}}})$ [20, 30]. The function $C(g)$ relates the couplings in the 3 flavour and pure gauge theory in the $\overline{\text{MS}}$ scheme as,

$$[\bar{g}_{\overline{\text{MS}}}^{(0)}(m_\star)]^2 = C(\bar{g}_{\overline{\text{MS}}}(m_\star)) \bar{g}_{\overline{\text{MS}}}^2(m_\star), \quad (49)$$

and it is known to 4-loop order in perturbation theory [33–35].

Dividing eq. (47) on both sides by μ_{dec} yields eq. (25), which we rewrite here in a more precise form by including the power corrections from eq. (46),

$$\rho P(z/\rho) = \frac{\Lambda_{\overline{\text{MS}}}^{(0)}}{\Lambda_{\text{GF}}^{(0)}} \times \varphi_{\text{GF}}^{(0)}(\bar{g}_{\text{GF}}(\mu_{\text{dec}}, M)) + \mathcal{O}(\Lambda^2/M^2, \mu^2/M^2), \quad \rho \equiv \Lambda_{\overline{\text{MS}}}/\mu_{\text{dec}}. \quad (50)$$

⁴We refer the reader to Section 3.6 for a proper definition of M .

The scheme change $\Lambda_{\overline{\text{MS}}}^{(0)}/\Lambda_{\text{GF}}^{(0)} = 0.4981(17)$ [13] involves no approximation by virtue of eq. (13); we profit from the full accuracy of P in the $\overline{\text{MS}}$ scheme by working in terms of Λ -parameters.⁵

In [30] we computed the massive coupling $\bar{g}_{\text{GF}}^2(\mu_{\text{dec}}, M)$ for values of the quark masses⁶

$$M/\mu_{\text{dec}} \approx 4, 6, 8, 10, 12. \quad (51)$$

The determination of $\bar{g}_{\text{GF}}^2(\mu, M)$ requires a continuum extrapolation of the corresponding lattice estimates at non-zero lattice spacing. These extrapolations are difficult. On the one hand, solid continuum extrapolations require $aM \ll 1$. On the other hand, large values of M are needed in order to have small $\mathcal{O}(1/M^2)$ corrections in eq. (50). This multi scale problem can only be solved by employing large lattices in a finite volume scheme. These schemes avoid in fact the introduction of any additional scale since $\mu = 1/L$ (see [29, 30] for the details).

An additional problem in performing these continuum extrapolation is the presence of linear aM cutoff effects. The most critical ones to deal with originate from a term $\sim aM \text{tr} F^2$ in the Symanzik effective theory, which describes the expansion of lattice observables in powers of the lattice spacing a [36–40], accompanied by (non-integer) powers of $\alpha(1/a)$ [15, 41–44]. The $\sim aM \text{tr} F^2$ term can be removed by a proper change of the bare coupling g_0 as one varies the quark mass [40]. More precisely, when computing the mass-dependence of an observable such as $\bar{g}_{\text{GF}}^2(\mu, M)$, the quantity to keep fixed in order to have a fixed lattice spacing a is $\tilde{g}_0^2 = g_0^2(1 + b_g(\tilde{g}_0^2)am_q)$ rather than g_0 . This guarantees that the $\mathcal{O}(aM)$ effects due to the $\sim aM \text{tr} F^2$ term are absent in continuum extrapolations.⁷

Until recently, the improvement parameter $b_g(\tilde{g}_0^2)$ was only known to leading order in perturbation theory [45]. This approximation was used in our previous work [30]. Our error included an estimate of the effect that the difference between the (at the time unknown) non-perturbative value of b_g and its 1-loop approximation could have on the values of the coupling at finite lattice spacing. This estimate dominated the uncertainty of the continuum extrapolation of the massive couplings $\bar{g}_{\text{GF}}^2(\mu, M)$. In particular, this source of uncertainty was systematic and could only be estimated through perturbative arguments. Below we shall rely on our recent non-perturbative determination of b_g [14] in order to obtain precise continuum extrapolations of the massive coupling $\bar{g}_{\text{GF}}^2(\mu_{\text{dec}}, M)$ free of this systematic uncertainty.

3.4.1 Continuum limit of the massive couplings

We start with a precise definition of the massive coupling. The Gradient Flow coupling is defined with Schrödinger Functional boundary conditions as [8]

$$\bar{g}_{\text{GFT}}^2(\mu, M) = \frac{1}{\hat{\mathcal{N}}(t, a/L)} t^2 \langle E(t, x) \rangle \Big|_{T=2L, x_0=T/2, \sqrt{8t}=0.36 L}, \quad (52)$$

⁵We note that section 3.8 contains a perturbative analysis of the decoupling strategy based on eq. (50). This may provide the reader with a different and useful perspective on the general ideas presented in this and the following sections.

⁶A more precise definition of the massive coupling that we considered is given in the following sections.

⁷The Symanzik effective theory also predicts a term $\sim aM^2 \bar{\psi}\psi$. This, however, can be easily removed through a proper definition of the RGI quark mass M (see section 3.6 for more details).

where $E(t, x)$ is the energy density of the flow fields and $\hat{\mathcal{N}}$ a normalization constant. We focus on the preferred value $c = 0.36$ for $c = \sqrt{8t}/L$, but we thoroughly checked that different choices, $c \in \{0.30, 0.33, 0.36, 0.39, 0.42\}$, lead to completely equivalent results for $\Lambda_{\overline{\text{MS}}}^{(3)}$. Note the choice $T = 2L$, where T is the time extent of our space-time lattices. It defines the $x = \text{GFT}$ scheme, which is employed only for the massive coupling, while everywhere else, e.g. in the definition of μ_{dec} , the $x = \text{GF}$ scheme with $c = 0.3$ and $T = L$ is used. A non-perturbative matching of the two schemes will be discussed below. The primary reason for having $T = 2L$ for the massive coupling is that with this choice boundary effects $\propto 1/M$ are suppressed to a level well below our statistical uncertainties (see section 3.7 for details).

Couplings on lines of constant physics

The massive couplings are needed at fixed $L = 1/\mu_{\text{dec}}$ and for several values of the RGI mass M . Furthermore, the simulations employ a certain resolution a/L . The dimensionless quantities defining μ_{dec} and M are $\bar{g}_{\text{GF}}^2(\mu_{\text{dec}}) = 3.949$ and $z = M/\mu_{\text{dec}} = ML$, where it is understood that $\bar{g}_{\text{GF}}^2(\mu_{\text{dec}})$ is defined for $M = 0$, i.e. for a bare subtracted mass $m_{\text{q}} = 0$. As determined in [30], the bare couplings \tilde{g}_0^2 listed in table 2 ensure $\bar{g}_{\text{GF}}^2(\mu_{\text{dec}}) = 3.949$. The necessary values of m_{q} then follow from $aM = z \times a/L$ and the ALPHA-collaboration's work on the non-perturbative quark mass renormalization, which we summarize in section 3.6. Given am_{q} , one needs to perform the massive simulations with bare couplings g_0^2 such that the improved bare coupling $\tilde{g}_0^2 = (1 + b_{\text{g}}(\tilde{g}_0^2)am_{\text{q}})g_0^2$ is kept fixed. As discussed earlier, the improvement coefficient b_{g} is needed to cancel linear a -effects when connecting the theories at different masses, but fixed lattice spacing. For our range of \tilde{g}_0^2 , the non-perturbative b_{g} is given by [14]

$$b_{\text{g}}(\tilde{g}_0^2) = b_{\text{g}}^{(1)}\tilde{g}_0^2 - 0.0151\tilde{g}_0^4 + 0.0424\tilde{g}_0^6, \quad b_{\text{g}}^{(1)} = 0.036. \quad (53)$$

However, our simulations were performed when only the 1-loop approximation $b_{\text{g}} = 0.036\tilde{g}_0^2 + \mathcal{O}(\tilde{g}_0^4)$ was available. We deal with this mismatch by correcting the data for $\bar{g}_{\text{GFT}}^2(\mu_{\text{dec}}, M)$ in Table 2 of [30] for the change in the bare coupling due to the change in b_{g} via

$$\bar{g}_{\text{GFT,corrected}}^2(\mu_{\text{dec}}, M) = \bar{g}_{\text{GFT}}^2(\mu_{\text{dec}}, M) - \frac{d\bar{g}_{\text{GFT}}^2(\mu_{\text{dec}}, M)}{d\tilde{g}_0^2} \Delta b_{\text{g}} \tilde{g}_0^2 am_{\text{q}}. \quad (54)$$

The straightforward $\Delta b_{\text{g}} = b_{\text{g}}(\tilde{g}_0^2) - b_{\text{g}}^{(1)}\tilde{g}_0^2$ will be modified below.

As discussed in detail in [30], the derivative

$$\frac{d\bar{g}_{\text{GFT}}^2(\mu_{\text{dec}}, M)}{d\tilde{g}_0^2} = \frac{\bar{g}_{\text{GFT}}\beta_{\text{GFT}}^{(0)}(\bar{g}_{\text{GFT}})(1 - \eta^M(g_{\star}))}{\tilde{g}_0\beta_0^{(3)}(\tilde{g}_0)} [1 + R_{\text{z}} + R_{\text{a}}], \quad (55)$$

is known with uncertainties that affect the corrected couplings only well below their statistical uncertainties. Here we shall only quote the final expression for this derivative, but encourage the interested reader to consult the original references to

understand its derivation (see appendix D of [30] and references therein). We thus take

$$\beta_{\text{GFT}}^{(0)}(x) \approx -k_0 x^3, \quad (56)$$

$$1 - \eta^{\text{M}}(g_\star) \approx \frac{9}{11}, \quad (57)$$

$$\beta_0^{(3)}(x) \approx -0.054 x^3, \quad (58)$$

$$R_z \approx k_0 \frac{b}{z^2} \bar{g}_{\text{GFT}}^2, \quad (59)$$

$$R_a \approx \frac{p_1 + p_2 z^2}{\bar{g}_{\text{GFT}} \beta_{\text{GFT}}^{(0)}(\bar{g}_{\text{GFT}}) (1 - \eta^{\text{M}}(g_\star))} \left(\frac{a}{L}\right)^2, \quad (60)$$

where for the case $c = 0.36$ we have: $p_1 = -21.4, p_2 = 1.08, b = 10.54$, and $k_0 = 0.076$.

Beside the accuracy of the derivative (55) itself, we also need to worry about the size of the quadratic (and higher order) terms in Δb_g which are neglected in the linear approximation (54). We therefore want small Δb_g values. This can be achieved by adding to Δb_g a term which only modifies the $O((aM)^2)$ terms in $\bar{g}_{\text{GFT,corrected}}^2$, i.e. it is linear in aM ,

$$\Delta b_g = b_g(\tilde{g}_0^2) - b_g^{(1)} \tilde{g}_0^2 + c_{\text{M}} \times (aM). \quad (61)$$

As long as the linear approximation (54) remains accurate, the coefficient c_{M} can be chosen at will. As anticipated, its effect is just an additional cutoff effect of $O((aM)^2)$ in the massive couplings, which does not affect the continuum values. For $c_{\text{M}} = -0.2$ the shift in \bar{g}_{GFT} is very small for the data point with $L/a = 12$ and $z = 6$. This choice results in very small shifts also for all other lattices that are relevant for the continuum extrapolation. The maximum value of $|\Delta b_g|$ is 0.03 and the maximum shift $|\bar{g}_{\text{GF,corrected}}^2 - \bar{g}_{\text{GF}}^2|$ is 0.1. As a confirmation that the choice of c_{M} is not crucial, we repeated the entire analysis with $c_{\text{M}} = -0.1$ and $c_{\text{M}} = -0.3$, see table 2.

Continuum extrapolation

For the continuum extrapolation we consider the fit ansatz

$$\bar{g}_{\text{GFT}}^2(\mu_{\text{dec}}, M_i) = \bar{g}^2(z_i) + p_1 [\alpha_s(a^{-1})]^{\hat{\Gamma}_{\text{eff}}} a^2 \mu_{\text{dec}}^2 + p_2 [\alpha_s(a^{-1})]^{\hat{\Gamma}'_{\text{eff}}} (aM_i)^2, \quad (62)$$

where $\bar{g}^2(z_i), p_1, p_2$ are fit parameters and $\alpha_s \equiv \alpha_{\overline{\text{MS}}}^{(N_f=3)}$. The fit parameters $\bar{g}^2(z_i)$ are the desired continuum couplings. The fit function is a result of an analysis of the Symanzik effective theory in the limit of large M [30]. Dropping relative corrections of order $O(1/M^2)$ in the effective theory reveals that there are no cross-terms of the form $a^2 M \mu_{\text{dec}}$ and that there are global coefficients p_1, p_2 instead of individual terms $\tilde{p}_i a^2$ for each value of $z_i = M_i/\mu_{\text{dec}}$. Due to the expansion in $1/M$, the functional form eq. (62) is only expected to describe data at large values of M . For our case it is a very good approximation for $z = M/\mu_{\text{dec}} \geq 4$. Indeed, the slopes in the extrapolations in $(aM)^2$ in figure 7 (left) vary little with z .

Table 2 collects the data that is included in the global fit, as well as the results of the continuum extrapolations. We also give the continuum values for several choices

of the shift parameter c_M . As we can see from the results in the table, varying c_M in the range $-0.1, -0.3$ around our preferred value -0.2 results in variations of the continuum values of at most $1/3$ of the statistical uncertainties.

The effect of the non-perturbative knowledge of b_g is crucial for the accuracy of our continuum limits. Compared with our previous results of [30], our continuum data is now between three to four times more precise. It is also worth noting that after the correction the data is much more linear in a^2 . Judging by the quality of the fit alone, we could in fact extend the fitting range to include data up to $(aM)^2 \approx 0.3$ (and thus reduce the statistical uncertainties in the continuum even further). We however decided to quote as final result the fit that only includes data with $(aM)^2 < 0.16$. This approach is conservative, since it leads to larger uncertainties and entirely compatible central values. In addition, this choice keeps the effect of the logarithmic corrections in the continuum extrapolation under control. Varying the corresponding parameters in the relevant range: $\Gamma_{\text{eff}} \in [-1, 1]$ and $\Gamma'_{\text{eff}} \in [-1/9, 1]$, the effect that we observe is typically of about the same size as the statistical errors on the continuum values. As we shall discuss later, this effect is subdominant in $\Lambda_{\overline{\text{MS}}}^{(3)}$ and at most of the order of 10% of the statistical uncertainties on $\Lambda_{\overline{\text{MS}}}^{(3)}$ (cf. Figure 8).

In conclusion, we are able to obtain precise values for the massive coupling in the continuum, where the choice of different ansätze for the continuum extrapolations results in values for $\Lambda_{\overline{\text{MS}}}^{(3)}$ that vary much less than the statistical fluctuations.

3.4.2 The determination of $\Lambda_{\overline{\text{MS}}}^{(3)}$

In our strategy, eq. (50), $\Lambda_{\overline{\text{MS}}}^{(3)}$ is determined via the pure gauge running function $\varphi_{\text{GF}}^{(0)}(g)$ in the GF scheme. On the other hand, the systematic errors due to boundary effects in the Schrödinger Functional are much easier to control for the GFT coupling, eq. (52). The idea is therefore to first apply the decoupling relation, eq. (46), to the GFT coupling, and in a second step switch to the GF scheme through the (pure gauge theory) function

$$\bar{g}_{\text{GF}}^{(0)}(\mu) = \chi_{0.36}(\bar{g}_{\text{GFT}}^{(0)}(\mu)). \quad (63)$$

Note that the scheme switch also involves the change in the value of c from $c = 0.36$ (GFT) to $c = 0.30$ (GF). (Other values for c in the GFT scheme have been considered for consistency checks.)

The precise form in which we apply the relation eq. (50) is thus the following,

$$\rho^{\text{eff}} P(z/\rho^{\text{eff}}) = \frac{\Lambda_{\overline{\text{MS}}}^{(0)}}{\Lambda_{\text{GF}}^{(0)}} \times \varphi_{\text{GF}}^{(0)}(\chi_{0.36}(\bar{g}_{\text{GFT}}(\mu_{\text{dec}}, M))), \quad \rho^{\text{eff}} \equiv \Lambda_{\overline{\text{MS}}}^{\text{eff}}/\mu_{\text{dec}}, \quad (64)$$

where we absorbed all power corrections of $O(1/M^2)$ into an effective Λ -parameter, $\Lambda_{\overline{\text{MS}}}^{\text{eff}}$. The latter needs to be extrapolated for $M \rightarrow \infty$ in order to extract the desired result, i.e.

$$\Lambda_{\overline{\text{MS}}} = \Lambda_{\overline{\text{MS}}}^{\text{eff}} + O(1/M^2). \quad (65)$$

We shall now turn to the details of the numerical analysis taking the continuum values for the massive coupling as input (cf. table 3).

The functions $\varphi_{\text{GF}}^{(0)}$ and $\chi_{0.36}$ can be determined from the results of [12] (see also appendix B of [30]). Here we list accurate numerical representations valid for the relevant couplings. The function $\chi_{0.36}$ is implicitly defined by its inverse function $\chi_{0.36}^{-1}$ via the expression

$$[\chi_{0.36}^{-1}(g)]^2 = \frac{g^2}{1 + g^2 P_{n_p}^{0.36}(g^2)}, \quad (66)$$

where $P_2^{0.36}$ is a second degree polynomial with coefficients

$$p_0 = -7.8231 \times 10^{-2}, \quad (67)$$

$$p_1 = 8.0579 \times 10^{-3}, \quad (68)$$

$$p_2 = -6.8506 \times 10^{-4}, \quad (69)$$

and covariance

$$\text{cov}(p_i, p_j) = \begin{pmatrix} +3.07343869 \times 10^{-4} & -1.35537879 \times 10^{-4} & +1.48252105 \times 10^{-5} \\ -1.35537879 \times 10^{-4} & +6.01436188 \times 10^{-5} & -6.58280673 \times 10^{-6} \\ +1.48252105 \times 10^{-5} & -6.58280673 \times 10^{-6} & +7.24967403 \times 10^{-7} \end{pmatrix}. \quad (70)$$

The polynomial is accurate for couplings $g^2 \in [3.8, 5.1]$.

The function $\varphi_{\text{GF}}^{(0)}(g)$ defined in eq. (8) determines the Λ -parameter in the pure gauge theory as a function of g in the GF scheme. We use the numerical representation

$$\begin{aligned} \varphi_{\text{GF}}^{(0)}(g) &= f_0 \\ &\times \exp \left\{ \frac{p_0}{2} \left(\frac{1}{g_{\text{sw}}^2} - \frac{1}{g^2} \right) + \frac{p_1}{2} \log \frac{g_{\text{sw}}^2}{g^2} + \frac{p_2}{2} (g_{\text{sw}}^2 - g^2) + \frac{p_3}{4} (g_{\text{sw}}^4 - g^4) \right\}, \end{aligned} \quad (71)$$

with parameters

$$g_{\text{sw}}^2 = 4\pi \times 0.2, \quad f_0 = 0.2658(36), \quad p_0 = 14.93613381, \quad (72)$$

$$p_1 = -1.03947429, \quad p_2 = 0.18007512, \quad p_3 = -0.01437036, \quad (73)$$

and covariance

$$\begin{aligned} \text{cov}(p_i, p_j) &= \\ &\begin{pmatrix} +5.24669327 \times 10^{-1} & -3.26120586 \times 10^{-1} & +6.03484522 \times 10^{-2} & -3.33454413 \times 10^{-3} \\ -3.26120586 \times 10^{-1} & +2.07627940 \times 10^{-1} & -3.91082685 \times 10^{-2} & +2.19046893 \times 10^{-3} \\ +6.03484522 \times 10^{-2} & -3.91082685 \times 10^{-2} & +7.47684098 \times 10^{-3} & -4.23948184 \times 10^{-4} \\ -3.33454413 \times 10^{-3} & +2.19046893 \times 10^{-3} & -4.23948184 \times 10^{-4} & +2.42972883 \times 10^{-5} \end{pmatrix}. \end{aligned} \quad (74)$$

These functions are applied to the second column of table 3 to determine columns three and four.

The $z \rightarrow \infty$ extrapolation of ρ^{eff} is carried out by a fit to the leading behavior in the large mass expansion,

$$\rho^{\text{eff}} = \rho + s [\alpha_s(m_\star)]^{\hat{\Gamma}_M} \frac{1}{z^2}, \quad (75)$$

where, we recall, m_\star is defined by $\bar{m}_{\overline{\text{MS}}}(m_\star) = m_\star$, and we vary $\hat{\Gamma}_M = 0, 1$. The results are found in table 3. Taking the more conservative fits to the data with $z \geq 6$ ($\hat{\Gamma}_M = 0$) we obtain

$$\rho = 0.4264(97). \quad (76)$$

The corresponding large mass extrapolation is shown in Figure 5.

We end this section with a remark on the different systematics that affect our computation. Despite the fact that we work in a finite volume, using very small values of the lattice spacing ($a^{-1} \approx 10 - 50$ GeV, with $\alpha_s(a^{-1})$ varying very little), the continuum values of the massive coupling are affected by the choice of $\hat{\Gamma}_{\text{eff}}, \hat{\Gamma}'_{\text{eff}}$ (cf. eq. (62)). This illustrates how difficult continuum extrapolations can be. Fortunately, our final goal is not the determination of the massive coupling in the continuum itself, but rather the determination of $\Lambda_{\overline{\text{MS}}}^{(3)}$. As figure 8 shows, the effect on $\Lambda_{\overline{\text{MS}}}^{(3)}$ due to the change in the coupling values for different continuum extrapolations is very mild. Logarithmic corrections in the $M \rightarrow \infty$ extrapolation (cf. the parameter $\hat{\Gamma}_M$ in eq. (75)) also have little effect on $\Lambda_{\overline{\text{MS}}}^{(3)}$. All in all, our decoupling strategy has allowed us to extract Λ with an error dominated by statistical uncertainties.

3.5 The strong coupling

The two strategies that we employed for extracting $\Lambda_{\overline{\text{MS}}}^{(3)}$ are largely independent, and are affected by very different systematics. First we quote the results of $\Lambda_{\overline{\text{MS}}}^{(3)}$ in units of $\sqrt{t_0}$ determined using each strategy

$$\text{Massless running: } \sqrt{8t_0} \times \Lambda_{\overline{\text{MS}}}^{(3)} = 0.712(21), \quad (77)$$

$$\text{Decoupling: } \sqrt{8t_0} \times \Lambda_{\overline{\text{MS}}}^{(3)} = 0.703(18). \quad (78)$$

Using our estimate for $\sqrt{t_0}$ (cf. section 3.1) we obtain:

$$\text{Massless running: } \Lambda_{\overline{\text{MS}}}^{(3)} = 347(11) \text{ MeV}, \quad (79)$$

$$\text{Decoupling: } \Lambda_{\overline{\text{MS}}}^{(3)} = 341.9(9.6) \text{ MeV}, \quad (80)$$

The results show a good agreement, with a correlation between the two estimates of $\Lambda_{\overline{\text{MS}}}^{(3)}$ of 6.5×10^{-5} . Since the uncertainties are dominated by statistics and have very different origin, an average is justified. A fit to a constant leads to our final result

$$\sqrt{8t_0} \times \Lambda_{\overline{\text{MS}}}^{(3)} = 0.707(15) \quad (81)$$

$$\Lambda_{\overline{\text{MS}}}^{(3)} = 343.8(8.4) \text{ MeV}. \quad (82)$$

All that is left to do now is to convert the result for $\Lambda_{\overline{\text{MS}}}^{(3)}$ into a value for the strong coupling. This is performed in two steps:

1. With $m_c^* = 1275.0(5.0)$ MeV and $m_b^* = 4171(20)$ MeV as values for the quark masses [23], we use perturbation theory to cross the charm and bottom thresholds:

$$\Lambda_{\overline{\text{MS}}}^{(5)} = P_{4,5}(M_b/\Lambda_{\overline{\text{MS}}}^{(5)}) \times P_{3,4}(M_c/\Lambda_{\overline{\text{MS}}}^{(4)}) \times \Lambda_{\overline{\text{MS}}}^{(3)}. \quad (83)$$

In this expression the P_{N_f, N_f+1} factors are the ratios of Λ parameters computed in perturbation theory after the decoupling of a single quark of mass M ,

$$P_{N_f, N_f+1}(M/\Lambda_{\overline{\text{MS}}}^{(N_f+1)}) = \frac{\Lambda_{\overline{\text{MS}}}^{(N_f+1)}}{\Lambda_{\overline{\text{MS}}}^{(N_f)}}. \quad (84)$$

2. Using the experimental input $m_Z = 91188.0(2.0)$ MeV [46] one determines $\alpha_s(m_Z)$ by solving the equation

$$\frac{\Lambda_{\overline{\text{MS}}}^{(5)}}{m_Z} = \varphi_{\overline{\text{MS}}}^{(N_f=5)} \left(\sqrt{\alpha_s(m_Z) \times (4\pi)} \right). \quad (85)$$

Both steps rely on perturbation theory and it is important to estimate the effect of the truncation of the perturbative series on the final result.

The second step carries negligible perturbative uncertainties thanks to the fact that m_Z is a very high energy scale and the β -function that enters the function $\varphi_{\overline{\text{MS}}}^{(N_f=5)}$ is known to 5-loop order. The evaluation of the factors $P_{3,4}, P_{4,5}$, on the other hand, requires to use perturbation theory at relatively low energy scales (the charm and bottom quark masses). These factors are also known in perturbation theory to 5-loop accuracy. The 3-, 4-, and 5-loop order terms of the product $P_{3 \rightarrow 5} = P_{3,4} \times P_{4,5}$ give contributions to $\alpha_s(m_Z)$ of 128×10^{-5} , 19×10^{-5} , and 6×10^{-5} , respectively. This shows that the perturbative series is well behaved, with fast decreasing contributions as the perturbative order is increased (see figure 9). We use the last term in the series as an estimate of the perturbative truncation errors. As a check we tried several variants of scale variations by a factor of two, using the explicit matching formulae from [33, 34], for either the running mass in the $\overline{\text{MS}}$ scheme at a given scale (3 GeV for charm, 4–5 GeV for the bottom-quark), or by varying the ratios μ/m_* (up and down for bottom and only up for the charm quark). In the first case, a scale-variation up and down, for both the coupling and the running quark mass, leads to uncertainties in $P_{3,4}$ and $P_{4,5}$ significantly smaller than our estimates. The only effect somewhat exceeding our estimate was found in $P_{4,5}$ when varying μ/m_* for the bottom quark, and corresponds to $(1.17 \text{ vs. } 0.84) \times 10^{-5}$ in $\alpha_s(m_Z)$.

The factor $P_{3 \rightarrow 5}$ also has non-perturbative contributions. These are more difficult to estimate. In [32] the simultaneous decoupling of 2 quarks was studied in detail. We use their estimate (0.2% in Λ per quark at the charm mass) with an increased uncertainty (due to a potential difference between the model $P_{0,2}$ and the physical case of QCD that is dominated by $P_{3,4}$), to add an additional 0.5% uncertainty to

$\Lambda_{\overline{\text{MS}}}^{(3)}$. These steps lead to our final value

$$\alpha_s(m_Z) = 0.11873(56) \quad [0.47\%]. \quad (86)$$

Our result is very precise, still the uncertainties are dominated by the uncertainty in $\Lambda_{\overline{\text{MS}}}^{(3)}$ (eq. (81)). The two main sources of uncertainty are the running in the pure gauge theory and the scale $\sqrt{t_0}$, each contributing approximately 25% to the error squared in $\alpha_s(m_Z)$. The massless running at high energies (eq. (44)) contributes 16% of the error squared, and the dimensionless ratio $\sqrt{t_0^*}\mu_{\text{had}}$ (eq. (30)) contributes 10%. The rest of the uncertainty in our final result comes from the statistical uncertainties in the determination of the massive couplings. Note that most of the sources of uncertainty are statistical. In particular both the non-perturbative and perturbative truncation errors in $P_{3\rightarrow 5}$ contribute each less than 2% to the total error squared. The perturbative uncertainties from the truncation of the function P entering the decoupling relation, eq. (64), are even smaller, and amount to only 1.7% of the final error squared of $\alpha_s(m_Z)$.

3.6 Mass renormalization

In the decoupling strategy, the continuum limit is taken at some prescribed values of the renormalization-group invariant (RGI) quark mass, $z = M/\mu_{\text{dec}} = 4, 6, \dots, 12$, measured in units of the scale μ_{dec} at which we apply decoupling (cf. Section 3.4). On the lattice, this is achieved by a proper tuning of the bare quark-mass parameter m_0 appearing in the lattice Lagrangian as a function of the lattice cutoff $1/a$. More precisely, for the lattice discretization employed in this work, the relation between the RGI and bare quark mass reads⁸

$$M = Z_M(\tilde{g}_0^2)\tilde{m}_q, \quad \tilde{m}_q = m_q(1 + b_m(\tilde{g}_0^2)am_q), \quad m_q = m_0 - m_{\text{crit}}. \quad (87)$$

In this equation, $Z_M(\tilde{g}_0^2)$ is the renormalization factor that relates the so called improved bare subtracted quark mass \tilde{m}_q and the RGI mass M . It only depends on the value of the lattice cutoff through \tilde{g}_0^2 , while, as M itself, it is renormalization scheme and scale independent. The coefficient function $b_m(\tilde{g}_0^2)$ appearing in \tilde{m}_q is analogous to the function $b_g(\tilde{g}_0^2)$ entering the definition of the improved bare coupling \tilde{g}_0^2 : if properly tuned, it allows for the removal of $O(a)$ discretization errors in the definition of the renormalized quark mass [40].⁹ Given $b_m(\tilde{g}_0^2)$, the improved mass \tilde{m}_q is related to the subtracted quark mass m_q by a quadratic equation. The bare mass m_q is defined in terms of the parameter m_0 that controls the simulations and the critical mass parameter $m_{\text{crit}} \equiv m_{\text{crit}}(g_0^2)$, which identifies the value of m_0 for which (up to discretization errors) the quarks are massless.

In ref. [30], the functions $Z_M(\tilde{g}_0^2)$, $b_m(\tilde{g}_0^2)$, and $m_{\text{crit}}(g_0^2)$, have been determined for the values of the lattice spacing of interest from the results for Z_m , b_m , and am_{crit}

⁸We recall that \tilde{g}_0^2 stands for the so called improved bare coupling (cf. Section 3.4) and a given value of \tilde{g}_0^2 corresponds to a particular value of the lattice cutoff $1/a$.

⁹We note that differently from ref. [40], we take as an argument of the function b_m the improved bare coupling \tilde{g}_0^2 instead of g_0^2 . The difference between these two choices amounts to an $O((am_q)^2)$ effect in M .

L/a	β	am_{crit}	Z_{m}	b_{m}
12	4.3020	-0.323417(38)	1.6882(72)	-0.42(20)
16	4.4662	-0.312928(23)	1.7252(80)	-0.50(12)
20	4.5997	-0.304289(24)	1.739(10)	-0.47(14)
24	4.7141	-0.296941(14)	1.770(11)	-0.51(10)
32	4.9000	-0.285427(12)	1.813(17)	-0.619(48)
40	5.0671	-0.275473(11)	1.807(19)	-0.50(10)
48	5.1739	-0.2693605(82)	1.823(22)	-0.528(73)

Table 4: Results for am_{crit} , $Z_{\text{m}} \equiv Z_{\text{m}}^{\text{SF}}(g_0^2, a\mu_{\text{dec}})$, and b_{m} , for different values of L/a and $\beta = 6/g_0^2$. See the main text for any unexplained notation.

collected in Table 4. The renormalization factor Z_{M} is determined via the introduction of an intermediate, mass-independent, renormalization scheme r for the quark mass, according to the equation

$$Z_{\text{M}}(\tilde{g}_0^2) = \left(\frac{M}{\bar{m}_r(\mu_{\text{dec}})} \right) Z_{\text{m}}^r(\tilde{g}_0^2, a\mu_{\text{dec}}). \quad (88)$$

In this equation, we denoted with $Z_{\text{m}}^r(\tilde{g}_0^2, a\mu_{\text{dec}})$ the renormalization constant that defines the corresponding renormalized, running, quark mass,

$$\bar{m}_r(\mu_{\text{dec}}) = \lim_{a \rightarrow 0} Z_{\text{m}}^r(\tilde{g}_0^2, a\mu_{\text{dec}}) \tilde{m}_{\text{q}}, \quad (89)$$

in the renormalization scheme r and at the renormalization scale $\mu = \mu_{\text{dec}}$.

In order to compute the first factor on the r.h.s. of eq. (88), one needs to determine, in the continuum limit, the RG evolution of the quark mass $\bar{m}_r(\mu)$ from the scale μ_{dec} , up to infinite energy. The RG running of the quark mass is encoded in the function $\varphi_{r,\text{m}}(\bar{g}_s)$ that defines the RGI quark mass through,¹⁰

$$M = \bar{m}_r(\mu) \varphi_{r,\text{m}}(\bar{g}_s(\mu)), \quad (90)$$

$$\varphi_{r,\text{m}}(\bar{g}_s) = [2b_0\bar{g}_s^2]^{-\frac{d_0}{2b_0}} \exp \left\{ - \int_0^{\bar{g}_s} \left[\frac{\tau_r(x)}{\beta_s(x)} - \frac{d_0}{b_0 x} \right] dx \right\}. \quad (91)$$

Here β_s is the RG-function of the gauge coupling in the scheme s introduced earlier (cf. eq. (5)), while

$$\tau_r(\bar{g}_s(\mu)) = \frac{d \ln \bar{m}_r(\mu)}{d \ln \mu}, \quad (92)$$

¹⁰For the ease of notation we label the function $\varphi_{r,\text{m}}(\bar{g}_s)$ only with the scheme r defining the renormalized quark masses, although implicitly its form depends also on the scheme s chosen for its argument, the gauge coupling. The same is true for the τ -function. On the other hand, note that if either of these functions is expressed as a function of the renormalization scale μ in physical units, rather than the coupling \bar{g}_s^2 , they only depend on r (cf. e.g. ref. [48]).

determines the scale dependence of the quark mass in the scheme r . At high energy, $\mu \rightarrow \infty$, the function $\tau_r(\bar{g}_s(\mu))$ admits a perturbative expansion in powers of \bar{g}_s^2 , where the leading order coefficient d_0 is scheme independent, i.e.

$$\tau_r(\bar{g}_s) \stackrel{\bar{g}_s \rightarrow 0}{\sim} -\bar{g}_s^2(d_0 + d_1^{r,s}\bar{g}_s^2 + \dots), \quad d_0 = 6C_F/(4\pi)^2. \quad (93)$$

From these definitions it is easy to show that the RGI mass M is renormalization scheme and scale independent and, thus, satisfies,

$$M = \bar{m}_r(\mu)\varphi_{r,m}(\bar{g}_s(\mu)) = \bar{m}_{r'}(\mu')\varphi_{r',m}(\bar{g}_{s'}(\mu')). \quad (94)$$

We moreover note that from eq. (90), it is immediate to infer that the ratio of quark masses at two different scales, μ_1, μ_2 , can be written as

$$\frac{\bar{m}_r(\mu_2)}{\bar{m}_r(\mu_1)} = \exp \left\{ \int_{\bar{g}_s(\mu_1)}^{\bar{g}_s(\mu_2)} \frac{\tau_r(x)}{\beta_s(x)} dx \right\}. \quad (95)$$

Similarly to the determination of the Λ -parameter (cf. Sects. 1.1 and 1.2), also the ratio $M/\bar{m}_r(\mu_{\text{dec}})$ is obtained by breaking up the computation of the RG running of the quark masses into two separate factors, each one referring to a different energy range,

$$\frac{M}{\bar{m}_r(\mu_{\text{dec}})} = \frac{M}{\bar{m}_r(\mu_0/2)} \times \frac{\bar{m}_r(\mu_0/2)}{\bar{m}_r(\mu_{\text{dec}})}, \quad (96)$$

where $\mu_0 = 4381(93)$ MeV is the renormalization scale already introduced in Sect. 1.2.

For the first term in eq. (96), we find [48],

$$\frac{M}{\bar{m}_{\text{SF}}(\mu_0/2)} = 1.7505(89). \quad (97)$$

The determination relies on finite-volume renormalization schemes for both the quark masses and the gauge coupling based on the Schrödinger functional (SF) of QCD. It is obtained by considering eq. (90) and the following parameterizations for the RG-functions [48],

$$\tau_{\text{SF}}(\bar{g}_{\text{SF}}) = -\bar{g}_{\text{SF}}^2 \sum_{n=0}^2 d_n \bar{g}_{\text{SF}}^{2n} \quad \beta_{\text{SF}}(\bar{g}_{\text{SF}}) = -\bar{g}_{\text{SF}}^3 \sum_{n=0}^3 b_n \bar{g}_{\text{SF}}^{2n} \quad \bar{g}_{\text{SF}}^2 \in [0, 2.45] \quad (98)$$

where the coefficients b_0, b_1, b_2 , and d_0, d_1 are fixed to their perturbative values, with

$$d_1^{\text{SF}} = \frac{1}{(4\pi)^2}(0.2168 + 0.084N_f), \quad (99)$$

$$b_2^{\text{SF}} = \frac{1}{(4\pi)^3}(0.483 - 0.275N_f + 0.0361N_f^2 - 0.00175N_f^3), \quad (100)$$

scheme dependent, while

$$(4\pi)^3 d_2^{\text{fit}} = -0.18(52), \quad (4\pi)^4 b_3^{\text{fit}} = 4(3), \quad (101)$$

were inferred from the data. The value of the gauge coupling corresponding to the scale $\mu = \mu_0/2$ is given instead by (remember that μ_0 was defined by $\bar{g}_{\text{SF}}^2(\mu_0) = 2.012$) [2],

$$\bar{g}_{\text{SF}}^2(\mu_0/2) = 2.452(11). \quad (102)$$

For the second factor in eq. (96), we find,

$$\frac{\bar{m}_{\text{SF}}(\mu_0/2)}{\bar{m}_{\text{SF}}(\mu_{\text{dec}})} = 0.8423(23). \quad (103)$$

It is obtained considering eq. (95) and the following parameterization of the ratio of RG-functions [48]

$$\frac{\tau_{\text{SF}}(\bar{g}_{\text{GF}})}{\beta_{\text{GF}}(\bar{g}_{\text{GF}})} = \frac{1}{\bar{g}_{\text{GF}}} \sum_{n=0}^3 f_n \bar{g}_{\text{GF}}^{2n}, \quad (104)$$

with

$$f_0 = 1.28493, \quad f_1 = -0.292465, \quad f_2 = 0.0606401, \quad f_3 = -0.00291921. \quad (105)$$

These parameters are correlated with covariance,

$$\text{cov}(f_i, f_j) = \begin{pmatrix} 2.33798 \times 10^{-2} & -1.47011 \times 10^{-2} & 2.81966 \times 10^{-3} & -1.66404 \times 10^{-4} \\ -1.47011 \times 10^{-2} & 9.54563 \times 10^{-3} & -1.87752 \times 10^{-3} & 1.12962 \times 10^{-4} \\ 2.81966 \times 10^{-3} & -1.87752 \times 10^{-3} & 3.78680 \times 10^{-4} & -2.32927 \times 10^{-5} \\ -1.66404 \times 10^{-4} & 1.12962 \times 10^{-4} & -2.32927 \times 10^{-5} & 1.46553 \times 10^{-6} \end{pmatrix}. \quad (106)$$

The relevant values of the gauge coupling are given by (cf. section 3.2 and [4, 30]),

$$\bar{g}_{\text{GF}}^2(\mu_0/2) = 2.6723(64), \quad \bar{g}_{\text{GF}}^2(\mu_{\text{dec}}) = 3.949. \quad (107)$$

Combining the results above, we finally obtain,

$$\frac{M}{\bar{m}_{\text{SF}}(\mu_{\text{dec}})} = 1.4744(85). \quad (108)$$

We refer the interested reader to [30] and references therein for more details on the determinations presented in this section.

We conclude by noticing that our analysis properly takes into account the uncertainties on Z_m , b_m , am_{crit} (and their correlation) as well as those on $M/\bar{m}_{\text{SF}}(\mu_{\text{dec}})$ in the determination of $z = M/\mu_{\text{dec}}$. These errors are propagated to the massive coupling $\bar{g}_{\text{GF}}^2(\mu_{\text{dec}}, M)$ and finally to our result for $\Lambda_{\overline{\text{MS}}}^{(3)}$ from decoupling. The uncertainty on z contributes less than a 0.5% to the final error squared of $\Lambda_{\overline{\text{MS}}}^{(3)}$, eq. (3).

3.7 Boundary contributions to the decoupling limit

The GF coupling with SF boundary conditions employed in our decoupling strategy (cf. eq. (52)) is in principle affected by $O(1/M)$ corrections to the large-mass limit. We can obtain an explicit expression for these contributions by invoking the tools of effective field theory.

3.7.1 Effective decoupling theory and $O(1/M)$ terms

Focusing on the continuum theory, at large quark mass, QCD with N_f mass-degenerate quarks can be described by an effective theory with action [32, 49],

$$S_{\text{dec}} = S_{0,\text{dec}} + \frac{1}{m} S_{1,\text{dec}} + \frac{1}{m^2} S_{2,\text{dec}} + \dots, \quad (109)$$

where for the time being m refers to a generic quark mass to be specified later. Since all quarks decouple simultaneously, the leading term $S_{0,\text{dec}}$ corresponds to the pure gauge action,

$$S_{0,\text{dec}} = -\frac{1}{2g^2} \int d^4x \operatorname{tr}(F_{\mu\nu} F_{\mu\nu}), \quad (110)$$

where $F_{\mu\nu}$ is the Yang-Mills field-strength tensor and g a yet unspecified gauge coupling. The other terms, $S_{k,\text{dec}}$ with $k > 0$, are given by space-time integrals of gauge invariant local operators, polynomial in the gauge field and its derivatives. In the case of a theory with no space-time boundary these are of mass dimension $4 + k$. Moreover, gauge invariance and $O(4)$ symmetry do not allow for odd values of k , so that the $S_{1,\text{dec}}$ term must vanish.

Different is the situation in the presence of SF boundary conditions [1, 5]. In this case, additional terms are allowed in the effective action (109). The $S_{k,\text{dec}}$ terms can in fact include also space integrals of dimension $3 + k$ operators localized at $x_0 = 0, T$. Considering the homogeneous SF boundary conditions employed in our strategy and the symmetries of the resulting theory, one can show that we can now have a linear term in $1/m$ of the form [30]

$$S_{1,\text{dec}} = \int d^3x \omega_b(g) [\mathcal{O}_b(0, \mathbf{x}) + \mathcal{O}_b(T, \mathbf{x})], \quad \mathcal{O}_b(x) = -\frac{1}{g^2} \sum_{k=1}^3 \operatorname{tr}(F_{0k}(x) F_{0k}(x)). \quad (111)$$

In this equation, $\omega_b(g)$ is a coefficient function that needs to be properly adjusted in order to match the results of QCD with N_f heavy quarks and those of the effective theory up to $O(1/m^2)$ corrections. Its value has been computed at 1-loop order in perturbation theory in ref. [30], and it is given by¹¹

$$\omega_b(g) = \omega_b^{(1)} g^2 + \omega_b^{(2)} g^4 + \dots, \quad \omega_b^{(1)} = -0.0541(5) N_f / (4\pi). \quad (112)$$

In the case of the GF coupling, the knowledge of the effective action is a crucial requirement to estimate the $O(1/m)$ corrections to its large-mass limit. Following the

¹¹Clearly, the value of the leading order coefficient $\omega_b^{(1)}$ does not depend on the choice of coupling g , which is yet unspecified.

discussion in ref. [30], we can in fact write,

$$\begin{aligned} \bar{g}_{\text{GFT}}^2(\mu, M) &\stackrel{M \rightarrow \infty}{=} [\bar{g}_{\text{GFT}}^{(0)}(\mu)]^2 - \\ &+ \frac{\omega_{\text{b}}(g_{\star})}{m_{\star}} \int d^3x \left\langle \frac{t^2 E(t, y)}{\mathcal{N}} [\mathcal{O}_{\text{b}}(0, \mathbf{x}) + \mathcal{O}_{\text{b}}(T, \mathbf{x})] \right\rangle_{\text{YM}}^{\text{conn}} + \mathcal{O}\left(\frac{1}{m_{\star}^2}\right). \end{aligned} \quad (113)$$

In the above equation $\langle \dots \rangle_{\text{YM}}^{\text{conn}}$ stands for the connected expectation value in the Yang-Mills theory with action $S_{0, \text{dec}}$, in the presence of homogeneous SF boundary conditions, and geometry $T = 2L$. The coupling $g_{\star} = \bar{g}_{\overline{\text{MS}}}(m_{\star})$ and quark mass $m_{\star} = \bar{m}_{\overline{\text{MS}}}(m_{\star})$ are those of the N_{f} -flavour theory, while the energy density $E(t, y)$ is evaluated for $\sqrt{8t} = cL$ and $y_0 = T/2$ (cf. Sect. 3.4.1).

3.7.2 Leading order estimate of the $\mathcal{O}(1/M)$ corrections

We can obtain an estimate for the size of the $\mathcal{O}(1/m)$ term in eq. (113) using lattice simulations [30]. To this end, we define the difference,

$$\Delta(z) \equiv \bar{g}_{\text{GFT}}^2(\mu_{\text{dec}}, M) - [\bar{g}_{\text{GFT}}^{(0)}(\mu_{\text{dec}})]^2, \quad z = M/\mu_{\text{dec}}. \quad (114)$$

Given eq. (113) and the leading order (LO) result, eq. (112), for the matching coefficient ω_{b} , we can write the LO estimate for the $\mathcal{O}(1/M)$ corrections to the massive GFT coupling as,

$$\Delta(z)|_{\text{LO}} \approx \frac{\omega_{\text{b}}^{(1)} g_{\star}^2}{z} \left(\frac{M}{m_{\star}}\right) p_1 (\bar{g}_{\text{GFT}}^2(\mu_{\text{dec}}, M)) + \mathcal{O}\left(g_{\star}^4, \frac{1}{z^2}\right). \quad (115)$$

Because $g_{\star} \rightarrow 0$ for $M \rightarrow \infty$, this estimate becomes more accurate the larger M is, since eq. (112) becomes a better approximation to ω_{b} . The coefficient function p_1 is given by the matrix element,

$$p_1 \equiv - \lim_{a \rightarrow 0} \int d^3x \left\langle \frac{t^2 E(t, y)}{\mathcal{N}} L [\mathcal{O}_{\text{b}}(0, \mathbf{x}) + \mathcal{O}_{\text{b}}(T, \mathbf{x})] \right\rangle_{\text{YM}}^{\text{conn}}. \quad (116)$$

This must be computed, non-perturbatively, along a line of constant physics defined by a fixed value of $\bar{g}_{\text{GFT}}^{(0)}(\mu_{\text{dec}}) \equiv \bar{g}_{\text{GFT}}(\mu_{\text{dec}}, M)$.

For the lattice computation of p_1 we followed the strategy described in ref. [30]. We refer the interested reader to this reference for the details on the lattice set-up, and in particular for a discussion on the lattice discretization of the relevant operators. We performed simulations for $L/a = 10, 12, 16$, at 3 or 4 values of β depending on the value of L/a . The values of β were chosen in such a way that p_1 can be interpolated in β so that the continuum limit can be taken at fixed $\bar{g}_{\text{GFT}}^{(0)}(\mu_{\text{dec}})$ corresponding to $\bar{g}_{\text{GFT}}(\mu_{\text{dec}}, M)$ with $z = 6$ and $c = 0.3, 0.36, 0.4$. The results for p_1 we obtained are collected in Table 5 for the 3 different lattice resolutions. We also provide an estimate of the continuum limit from linear extrapolations in a/L .

c	$\bar{g}_{\text{GF}}^2(\mu_{\text{dec}}, M)$	L/a	p_1
0.3	4.448	10	-0.396(62)
		12	-0.370(73)
		16	-0.305(49)
		∞	-0.15(17)
0.36	5.347	10	-0.94(10)
		12	-0.86(12)
		16	-0.77(07)
		∞	-0.48(26)
0.42	6.690	10	-2.06(17)
		12	-1.88(20)
		16	-1.71(12)
		∞	-1.14(43)

Table 5: Results for p_1 at finite lattice spacing. Estimates of $a/L \rightarrow 0$ extrapolations linear in a/L are also given.

Given the non-perturbative results for p_1 , all that is needed to compute $\Delta(z)|_{\text{LO}}$ are the values for g_* and M/m_* at the relevant quark mass. The latter can be obtained once

$$\frac{M}{\Lambda_{\overline{\text{MS}}}^{(3)}} = z \times \frac{\mu_{\text{dec}}}{\Lambda_{\overline{\text{MS}}}^{(3)}}, \quad (117)$$

is specified, thanks to the perturbative knowledge of the RG functions in the $\overline{\text{MS}}$ scheme [33–35, 50–58]. Taking $\mu_{\text{dec}}/\Lambda_{\overline{\text{MS}}}^{(3)} \approx 2.3$ and $z = 6$, we find for $N_f = 3$,

$$g_*^2 \approx 3.0277, \quad M/m_* \approx 1.4889, \quad (118)$$

where the 5-loop $\beta_{\overline{\text{MS}}}$ and 4-loop $\tau_{\overline{\text{MS}}}$ functions were used.

c	$\bar{g}_{\text{GF}}^2(\mu_{\text{dec}}, M)$	$\Delta(z=6) _{\text{LO}}$
0.30	4.448(14)	0.0029
0.36	5.347(22)	0.0075
0.42	6.690(37)	0.0170

Table 6: Results for $\Delta(z)|_{\text{LO}}$ for $z = 6$ and different values of c .

In order to obtain a generous estimate for $\Delta(z)|_{\text{LO}}$ we consider the value of p_1 at $L/a = 16$. This gives a more conservative choice than taking the continuum limit values (cf. Table 5). The results for $\Delta(z)|_{\text{LO}}$ computed in this way are collected in Table 6. Comparing the results for $\Delta(z)|_{\text{LO}}$ with the statistical uncertainties on the corresponding massive coupling $\bar{g}_{\text{GF}}^2(\mu_{\text{dec}}, M)$, we see that the former range from being about a factor 4-5 smaller for $c = 0.30$, to ≈ 3 times smaller for $c = 0.36$, to ≈ 2 times smaller for $c = 0.42$. We conclude that these effects can be safely discarded

for our preferred choice, $c = 0.36$ and $z = 6$. They decrease further $\sim 1/z$ as we reach the decoupling limit.

3.8 Massive gradient flow coupling in perturbation theory

It is instructive to study the decoupling of heavy quarks at the lowest non-trivial order in perturbation theory. The discussion will give us some qualitative insight on the size of the leading corrections to the infinite quark-mass limit in computing the Λ -parameter via the decoupling method. Concomitantly, we hope that it will help the reader to better understand our strategy in simpler, perturbative, terms.

Unfortunately, there are no known perturbative results in QCD for the specific coupling definition we employed in our strategy, i.e. the GF coupling defined in a finite volume with SF boundary conditions; only the pure gauge part has been obtained so far [13]. There are, however, results for an infinite space-time volume [22, 59]. In the following we shall consider these in order to get a qualitative picture for our case. We note that in the limit where $c = \sqrt{8t}/L \rightarrow 0$, our coupling tends to the infinite volume one with corrections of $O(c^4)$.

3.8.1 One-loop GF coupling in infinite volume

We begin by considering the perturbative results of ref. [59] for the energy density at positive flow time $\langle t^2 E(t) \rangle$ (cf. eq. (36) of that reference). After a proper normalization by an overall constant, we readily obtain the perturbative expansion of the GF coupling at the 1-loop order and for finite quark masses,

$$\bar{g}_{\text{GF}}^2(\mu, \bar{m}(\mu)) = \bar{g}_s^2(\mu) + c_1(z) \bar{g}_s^4(\mu) + O(\bar{g}_s^6), \quad (119)$$

$$c_1(z) = (1.0978 + 0.0075 N_f)/(4\pi) - \frac{N_f}{24\pi^2} \Omega_1(z), \quad (120)$$

where $\mu = 1/\sqrt{8t}$, $\bar{g}_s^2 \equiv \bar{g}_{\overline{\text{MS}}}^2(\mu)$, and $z \equiv \bar{m}(\mu)/\mu$. Note that we restrict to the case of N_f mass-degenerate quarks with renormalized quark mass $\bar{m}(\mu)$. At this order in perturbation theory there is no need to specify a renormalization scheme for the mass, which is therefore left unspecified.

The function $\Omega_1(z)$, which encodes the mass dependence of the coupling, is given here for completeness,

$$\Omega_1(z) = 1 - \gamma_E - \ln(z^2/4) - z^2 + z^2 I(z), \quad (121)$$

where

$$I(z) = \frac{1}{2} \int_0^\infty dx e^{-x/4} \left(1 + \frac{x}{4z^2}\right) \left(1 - \frac{x}{2z^2}\right) \frac{u \ln u}{u^2 - 1}, \quad (122)$$

$$u = \frac{\sqrt{x + 4z^2} - \sqrt{x}}{\sqrt{x + 4z^2} + \sqrt{x}}.$$

In the following, we will mostly be interested in its limits for small and large values of z ,

$$\Omega_1(z) \rightarrow \begin{cases} -\frac{3}{2}z^2 + \mathcal{O}(z^4), \\ -2\ln z - h - \frac{8}{5z^2} + \mathcal{O}(z^{-4}), \end{cases} \quad (123)$$

with $h = \gamma_E + \frac{2}{3} - 2\ln 2$.

3.8.2 Renormalization group improved coupling in the one-loop model

Eq. (119) is a well behaved perturbative expansion for small z , where the coefficient function $c_1(z)$ remains finite. However, $c_1(z)$ diverges in the limit of large z and the expansion becomes useless. Renormalization group (RG) improvement removes such an issue (and has already been silently used, setting $\mu = 1/\sqrt{8t}$), but for large z a second scale appears and RG improvement is not generally applicable to our knowledge. One could resort to the effective theory at large z at the expense of having to patch up domains of small and large z . Instead, here, we give a full RG improved expression valid for all z . Since it employs a non-systematic approximation, we call this the one-loop model.

We start from the truncated RG equations

$$\mu \frac{d}{d\mu} \frac{1}{\bar{g}_{\text{GF}}^2} = 2b_0(N_f) + \frac{N_f}{24\pi^2} \left(\mu \frac{d}{d\mu} \right) \Omega_1(z), \quad (124)$$

$$\mu \frac{d}{d\mu} \bar{m} = 0, \quad (125)$$

where $b_0(N_f)$ is the universal lowest order coefficient of the perturbative expansion of the β -function for N_f -flavours. While in eq. (124) the one-loop term is taken along, in eq. (125) it is dropped. It only contributes via c_1 in eq. (119) and therefore is higher order, as we have remarked before. However, even in the massless case, one has to include the two-loop term in the β -function and the one-loop term in the mass anomalous dimension in order to get a systematic expansion of the Λ -parameter and the RGI mass in terms of the coupling, see eqs. (8, 9) and (91, 90). We do not do this here and therefore we use the term model, not approximation.

The truncated RG equations can be integrated exactly to obtain,

$$\frac{1}{\bar{g}_{\text{GF}}^2} = 2b_0(N_f) \ln(\mu/\Lambda_{\text{GF}}^{(N_f)}) + \frac{N_f}{24\pi^2} \Omega_1(z), \quad \bar{m}(\mu) = M, \quad (126)$$

where $\Lambda_{\text{GF}}^{(N_f)}$ is a conveniently chosen constant; taking $z \rightarrow 0$ (and $b_1 = d_0 = 0$ as fit for the model), we see that it is the Λ -parameter in the GF scheme for the N_f -flavour theory. In the same way, the constant M can be identified with the RGI mass or the running mass.

At large values of z , the quarks decouple. We thus expect that,

$$\frac{1}{\bar{g}_{\text{GF}}^2} \stackrel{z \rightarrow \infty}{\equiv} 2b_0(0) \ln(\mu/\Lambda_{\text{GF,dec}}^{(0)}) + \mathcal{O}(1/z^2), \quad (127)$$

for a properly chosen function $\Lambda_{\text{GF,dec}}^{(0)} \equiv \Lambda_{\text{GF,dec}}^{(0)}(\Lambda_{\text{GF}}^{(N_f)}, M)$ of the Λ -parameter of the N_f -flavour theory, $\Lambda_{\text{GF}}^{(N_f)}$, and of the RGI quark mass M . We call $\Lambda_{\text{GF,dec}}^{(0)}$ the Λ -parameter of the effective theory.

Taking into account the asymptotic limit of $\Omega_1(z)$ for large z (cf. eq. (123)),

$$\Omega_1(z) = -2 \ln(z) - h + \Omega_1^{\text{sub}}(z), \quad \Omega_1^{\text{sub}}(z) = \mathcal{O}(1/z^2), \quad (128)$$

we find

$$\frac{1}{\bar{g}_{\text{GF}}^2} \stackrel{z \rightarrow \infty}{\equiv} 2b_0(N_f) \ln(\mu/\Lambda_{\text{GF}}^{(N_f)}) - \frac{N_f}{24\pi^2} (2 \ln(z) + h) + \mathcal{O}(1/z^2) \equiv 2b_0(0) \ln(\mu/\Lambda_{\text{GF,dec}}^{(0)}), \quad (129)$$

and with

$$b_0(N_f) = b_0(0) - \frac{N_f}{24\pi^2}, \quad (130)$$

we infer the relation between the Λ -parameter of the N_f -flavour theory and that of the effective theory,

$$P_{\text{GF}} \equiv \frac{\Lambda_{\text{GF,dec}}^{(0)}}{\Lambda_{\text{GF}}^{(N_f)}} = \left(\frac{M}{\Lambda_{\text{GF}}^{(N_f)}} \right)^{\eta_0(N_f)} \exp\left(\frac{h\eta_0(N_f)}{2} \right), \quad \eta_0(N_f) = 1 - \frac{b_0(N_f)}{b_0(0)}. \quad (131)$$

This relation can also be obtained from the ratio of Λ -parameters in the $\overline{\text{MS}}$ -scheme, i.e. the function P in eq. (48), setting $b_i = d_{i-1} = 0$, $i > 0$ and changing to the GF scheme for both $\Lambda^{(0)}$ and $\Lambda^{(3)}$. Note that this scheme-change is a z -independent factor.

3.8.3 Leading $\mathcal{O}(1/z^2)$ corrections to the decoupling relation in the model

We can gain some insight into the leading order corrections to the decoupling relation by keeping the $\mathcal{O}(1/z^2)$ terms in the large z expansion of the function $\Omega_1(z)$ when establishing the relation eq. (129). Along the lines of our decoupling strategy we thus introduce effective Λ -parameters (cf. section 3.4.2), $\Lambda^{\text{eff}} \equiv \Lambda_{\text{GF}}^{(N_f),\text{eff}}$ and $\Lambda_{\text{dec}}^{\text{eff}} \equiv \Lambda_{\text{GF,dec}}^{(0),\text{eff}}$, for the N_f -flavour and effective theory respectively, through the

definitions

$$\begin{aligned}
\frac{1}{\bar{g}_{\text{GF}}^2} &= 2b_0(N_f) \ln(\mu/\Lambda) - \frac{N_f}{24\pi^2} (2 \ln(z) + h - \Omega_1^{\text{sub}}(z)), \\
&\equiv 2b_0(N_f) \ln(\mu/\Lambda^{\text{eff}}) - \frac{N_f}{24\pi^2} (2 \ln(z) + h), \\
&\equiv 2b_0(0) \ln(\mu/\Lambda_{\text{dec}}^{\text{eff}}),
\end{aligned} \tag{132}$$

where for the ease of notation we also define $\Lambda \equiv \Lambda_{\text{GF}}^{(N_f)}$ and $\Lambda_{\text{dec}} \equiv \Lambda_{\text{GF,dec}}^{(0)}$. First note that, analogously to Λ and Λ_{dec} , the effective Λ -parameters are related by (cf. eqs. (129)-(131))¹²

$$\Lambda_{\text{dec}}^{\text{eff}} = P_{\text{GF}}(M/\Lambda^{\text{eff}}) \Lambda^{\text{eff}} = (M/\Lambda^{\text{eff}})^{\eta_0} e^{\frac{h\eta_0}{2}} \Lambda^{\text{eff}}. \tag{133}$$

Second, by construction, in the limit $z \rightarrow \infty$, Λ^{eff} and $\Lambda_{\text{dec}}^{\text{eff}}$ approach their respective counterparts Λ and Λ_{dec} with corrections of $O(1/z^2)$. In particular, from the definitions in eq. (132), we have that,

$$\ln(\Lambda^{\text{eff}}/\Lambda) = -\frac{\eta_0(N_f)}{2 - 2\eta_0(N_f)} \Omega_1^{\text{sub}}(z). \tag{134}$$

Considering the large z expansion of $\Omega_1(z)$ in eq. (123), this gives

$$\frac{\Lambda^{\text{eff}}}{\Lambda} = 1 + \frac{\eta_0(N_f)}{2 - 2\eta_0(N_f)} \frac{8}{5z^2} + O(1/z^4) \stackrel{N_f=3}{=} 1 + \frac{8}{45z^2} + O(1/z^4), \tag{135}$$

where the coefficient of the neglected $1/z^4$ term is of a similar size.

Considering that in our finite volume set-up $z = M/\mu = cML$, we find that, for $N_f = 3$, the above correction term is around 4% for $c = 0.36$ and $ML = 6$. Instead, if we use for M in the model the value of $\bar{m}(\mu)$ in the non-perturbative computation and use the non-perturbative relation $M/\bar{m}_{\text{SF}}(\mu_{\text{dec}}) \approx 1.47$, eq. (108), the effect we find is about two times larger. This level of ambiguity should not be surprising given the model used in our calculation; we recall that the coupling is computed only at one-loop order in perturbation theory (in infinite volume), and the running of the quark mass is neglected all-together. Nonetheless, the model captures the right bulk part of the effect. Looking at figure 5, that shows our non-perturbative results for Λ^{eff} , we see that for $c = 0.36$ and $ML = 6$ the correction is about 6% with respect to the infinite mass limit.

The result in eq. (135) also elucidates how the approach to the infinite mass limit can be tested when working at fixed L by considering different values of c . In particular, larger values of c are expected to lead to smaller corrections to the decoupling limit as

¹²In our strategy the Λ -parameters are first converted to the $\overline{\text{MS}}$ -scheme and the function $P_{\overline{\text{MS}}}$ is used. However, since the ratio $P_{\text{GF}}/P_{\overline{\text{MS}}}$ is independent of z , this change of schemes is irrelevant.

they effectively correspond to larger ratios M/μ .¹³ Following this reasoning, our final determination of Λ is based on the results for $c = 0.36$, which strikes a good balance between systematic and statistical uncertainties; both of them are small.

3.8.4 Illustration

The behavior of the coupling in the one loop model is shown in figure 2 (left) together with the massless coupling and the one in the decoupled theory with $\Lambda_{\text{GF,dec}}^{(0)}$ from eq. (131). The figure further illustrates the trajectory that one follows in the non-perturbative decoupling strategy.

Acknowledgments

We wish to express our gratitude to Martin Lüscher, Peter Weisz and Ulli Wolff, whose work on finite size scaling for renormalized couplings, the Schrödinger Functional and the gradient flow laid the foundations for the results presented here. We also thank them for numerous enlightening discussions and advice over the years. Furthermore, we are indebted to our colleagues in the ALPHA collaboration, especially Simon Kuberski, Patrick Fritsch, Jochen Heitger and Hubert Simma for sharing their data on the renormalized coupling. We thank Giulia Zanderighi for sharing the data that enters in Figure 1.

The work is supported by the Spanish MCIU project No. CNS2022-136005, the Generalitat Valenciana genT program No. CIDEGENT/2019/040, the German Research Foundation (DFG) research unit FOR5269 “Future methods for studying confined gluons in QCD”.

AR acknowledges financial support by the European projects H2020-MSCA-ITN-2019//860881-HIDDeN and 101086085-ASYMMETRY, and the national project PID2023-148162NB-C21. RH was supported by the programme “Netzwerke 2021”, an initiative of the Ministry of Culture and Science of the State of Northrhine Westphalia, in the NRW-FAIR network, funding code NW21-024-A. SS and RS acknowledge funding by the H2020 program in the Europlex training network, grant agreement No. 813942. Generous computing resources were supplied by the North-German Supercomputing Alliance (HLRN, project bep00072) and by the John von Neumann Institute for Computing (NIC) at DESY, Zeuthen, and the local SOM clusters, funded by the MCIU with funding from the European Union NextGenerationEU (PRTR-C17.I01) and Generalitat Valenciana Grant No. ASFAE/2022/020.

References

- [1] Lüscher, M., Narayanan, R., Weisz, P. & Wolff, U. The Schrödinger Functional: a renormalizable probe for non-abelian gauge theories. *Nucl.Phys.* **B384**, 168–228 (1992).
- [2] Dalla Brida, M. *et al.* A non-perturbative exploration of the high energy regime in $N_f = 3$ QCD. *Eur. Phys. J. C* **78**, 372 (2018).

¹³We recall that, instead, statistical uncertainties in \bar{g}_{GF}^2 and thus Λ^{eff} tend to increase for larger c -values.

- [3] Dalla Brida, M. *et al.* Determination of the QCD Λ -parameter and the accuracy of perturbation theory at high energies. *Phys. Rev. Lett.* **117**, 182001 (2016).
- [4] Dalla Brida, M. *et al.* Slow running of the Gradient Flow coupling from 200 MeV to 4 GeV in $N_f = 3$ QCD. *Phys. Rev.* **D95**, 014507 (2017).
- [5] Sint, S. On the Schrödinger functional in QCD. *Nucl.Phys.* **B421**, 135–158 (1994).
- [6] Bode, A., Weisz, P. & Wolff, U. Two loop computation of the Schrodinger functional in lattice QCD. *Nucl. Phys. B* **576**, 517–539 (2000). [Erratum: Nucl.Phys.B 608, 481–481 (2001), Erratum: Nucl.Phys.B 600, 453–453 (2001)].
- [7] Bruno, M. *et al.* QCD Coupling from a Nonperturbative Determination of the Three-Flavor Λ Parameter. *Phys. Rev. Lett.* **119**, 102001 (2017).
- [8] Fritzsche, P. & Ramos, A. The gradient flow coupling in the Schrödinger Functional. *JHEP* **1310**, 008 (2013).
- [9] Lüscher, M., Weisz, P. & Wolff, U. A Numerical method to compute the running coupling in asymptotically free theories. *Nucl.Phys.* **B359**, 221–243 (1991).
- [10] [RQCD 22] G. S. Bali *et al.* Scale setting and the light baryon spectrum in $N_f = 2 + 1$ QCD with Wilson fermions. *JHEP* **05**, 035 (2023).
- [11] Strassberger, B. *et al.* Scale setting for CLS 2+1 simulations. *PoS LATTICE2021*, 135 (2022).
- [12] Dalla Brida, M. & Ramos, A. The gradient flow coupling at high-energy and the scale of SU(3) Yang-Mills theory (2019).
- [13] Dalla Brida, M. & Lüscher, M. SMD-based numerical stochastic perturbation theory. *Eur. Phys. J. C* **77**, 308 (2017).
- [14] Dalla Brida, M. *et al.* Heavy Wilson Quarks and $O(a)$ Improvement: Nonperturbative Results for b_g (2023).
- [15] Husung, N., Marquard, P. & Sommer, R. Asymptotic behavior of cutoff effects in Yang-Mills theory and in Wilson’s lattice QCD. *Eur. Phys. J. C* **80**, 200 (2020).
- [16] [CalLat 20A] N. Miller *et al.* Scale setting the Möbius domain wall fermion on gradient-flowed HISQ action using the omega baryon mass and the gradient-flow scales t_0 and w_0 . *Phys. Rev. D* **103**, 054511 (2021).
- [17] [MILC 15] A. Bazavov *et al.* Gradient flow and scale setting on MILC HISQ ensembles. *Phys. Rev.* **D93**, 094510 (2016).
- [18] [HPQCD 13A] R. Dowdall, C. Davies, G. Lepage and C. McNeile. V_{us} from π and K decay constants in full lattice QCD with physical u , d , s and c quarks.

- Phys.Rev.* **D88**, 074504 (2013).
- [19] [RBC/UKQCD 14B] T. Blum *et al.* Domain wall QCD with physical quark masses. *Phys. Rev.* **D93**, 074505 (2016).
- [20] [ETM 21] C. Alexandrou *et al.* Ratio of kaon and pion leptonic decay constants with $N_f = 2 + 1 + 1$ Wilson-clover twisted-mass fermions. *Phys. Rev. D* **104**, 074520 (2021).
- [21] [BMW 12A] S. Borsanyi *et al.* High-precision scale setting in lattice QCD. *JHEP* **1209**, 010 (2012).
- [22] Lüscher, M. Properties and uses of the Wilson flow in lattice QCD. *JHEP* **08**, 071 (2010). [Erratum: *JHEP* 03, 092 (2014)].
- [23] Aoki, Y. *et al.* FLAG Review 2021. *Eur. Phys. J. C* **82**, 869 (2022).
- [24] Fritzsche, P., Heitger, J. & Kuberski, S. $\mathcal{O}(a)$ improved quark mass renormalization for a non-perturbative matching of HQET to three-flavor QCD. *PoS LATTICE2018*, 218 (2018).
- [25] Sommer, R. *et al.* A strategy for B-physics observables in the continuum limit. *PoS LATTICE2023*, 268 (2024).
- [26] Conigli, A. *et al.* m_b and $f_{B^{(*)}}$ in $2 + 1$ flavour QCD from a combination of continuum limit static and relativistic results. *PoS LATTICE2023*, 237 (2024).
- [27] Conigli, A. *et al.* B-physics observables in the continuum from a combination of static and relativistic results. *PoS EuroPLeX2023*, 005 (2024).
- [28] Bruno, M. & Sommer, R. On fits to correlated and auto-correlated data. *Comput. Phys. Commun.* **285**, 108643 (2023).
- [29] Dalla Brida, M. *et al.* Non-perturbative renormalization by decoupling. *Phys. Lett. B* **807**, 135571 (2020).
- [30] Dalla Brida, M. *et al.* Determination of $\alpha_s(m_Z)$ by the non-perturbative decoupling method. *Eur. Phys. J. C* **82**, 1092 (2022).
- [31] Nada, A. & Ramos, A. An analysis of systematic effects in finite size scaling studies using the gradient flow. *Eur. Phys. J. C* **81**, 1 (2021).
- [32] Athenodorou, A. *et al.* How perturbative are heavy sea quarks? *Nucl. Phys. B* **943**, 114612 (2019).
- [33] Chetyrkin, K. G., Kühn, J. H. & Sturm, C. QCD decoupling at four loops. *Nucl. Phys.* **B744**, 121–135 (2006).

- [34] Schröder, Y. & Steinhauser, M. Four-loop decoupling relations for the strong coupling. *JHEP* **01**, 051 (2006).
- [35] Gerlach, M., Herren, F. & Steinhauser, M. Wilson coefficients for Higgs boson production and decoupling relations to $\mathcal{O}(\alpha_s^4)$. *JHEP* **11**, 141 (2018).
- [36] Symanzik, K. Continuum Limit and Improved Action in Lattice Theories. 1. Principles and ϕ^4 Theory. *Nucl. Phys. B* **226**, 187–204 (1983).
- [37] Symanzik, K. Continuum Limit and Improved Action in Lattice Theories. 2. O(N) Nonlinear Sigma Model in Perturbation Theory. *Nucl. Phys. B* **226**, 205–227 (1983).
- [38] Lüscher, M. and Weisz, P. On-Shell Improved Lattice Gauge Theories. *Commun. Math. Phys.* **97**, 59 (1985). [Erratum: *Commun.Math.Phys.* 98, 433 (1985)].
- [39] Sheikholeslami, B. & Wohlert, R. Improved Continuum Limit Lattice Action for QCD with Wilson Fermions. *Nucl. Phys. B* **259**, 572 (1985).
- [40] Luscher, M., Sint, S., Sommer, R. & Weisz, P. Chiral symmetry and O(a) improvement in lattice QCD. *Nucl. Phys. B* **478**, 365–400 (1996).
- [41] Balog, J., Niedermayer, F. & Weisz, P. Logarithmic corrections to O(a²) lattice artifacts. *Phys. Lett. B* **676**, 188–192 (2009).
- [42] Balog, J., Niedermayer, F. & Weisz, P. The Puzzle of apparent linear lattice artifacts in the 2d non-linear sigma-model and Symanzik’s solution. *Nucl. Phys. B* **824**, 563–615 (2010).
- [43] Husung, N., Marquard, P. & Sommer, R. The asymptotic approach to the continuum of lattice QCD spectral observables. *Phys. Lett. B* **829**, 137069 (2022).
- [44] Husung, N. Logarithmic corrections to O(a) and O(a²) effects in lattice QCD with Wilson or Ginsparg–Wilson quarks. *Eur. Phys. J. C* **83**, 142 (2023). [Erratum: *Eur.Phys.J.C* 83, 144 (2023)].
- [45] Sint, S. & Sommer, R. The Running coupling from the QCD Schrodinger functional: A One loop analysis. *Nucl. Phys.* **B465**, 71–98 (1996).
- [46] Navas, S. *et al.* Review of particle physics. *Phys. Rev. D* **110**, 030001 (2024).
- [47] Herren, F. & Steinhauser, M. Version 3 of RunDec and CRunDec. *Comput. Phys. Commun.* **224**, 333–345 (2018).
- [48] Campos, I. *et al.* Non-perturbative quark mass renormalisation and running in $N_f = 3$ QCD. *Eur. Phys. J. C* **78**, 387 (2018).
- [49] Weinberg, S. Effective Gauge Theories. *Phys. Lett. B* **91**, 51–55 (1980).

- [50] Bernreuther, W. & Wetzel, W. Decoupling of Heavy Quarks in the Minimal Subtraction Scheme. *Nucl. Phys.* **B197**, 228–236 (1982). [Erratum: Nucl. Phys.B513,758(1998)].
- [51] Grozin, A. G. *et al.* Simultaneous decoupling of bottom and charm quarks. *JHEP* **09**, 066 (2011).
- [52] Kniehl, B. A., Kotikov, A. V., Onishchenko, A. I. & Veretin, O. L. Strong-coupling constant with flavor thresholds at five loops in the anti-MS scheme. *Phys. Rev. Lett.* **97**, 042001 (2006).
- [53] van Ritbergen, T., Vermaseren, J. A. M. & Larin, S. A. The Four loop beta function in quantum chromodynamics. *Phys. Lett.* **B400**, 379–384 (1997).
- [54] Czakon, M. The Four-loop QCD beta-function and anomalous dimensions. *Nucl. Phys.* **B710**, 485–498 (2005).
- [55] Baikov, P. A., Chetyrkin, K. G. & Kühn, J. H. Five-Loop Running of the QCD coupling constant. *Phys. Rev. Lett.* **118**, 082002 (2017).
- [56] Herzog, F., Ruijl, B., Ueda, T., Vermaseren, J. A. M. & Vogt, A. The five-loop beta function of Yang-Mills theory with fermions. *JHEP* **02**, 090 (2017).
- [57] Luthe, T., Maier, A., Marquard, P. & Schroder, Y. The five-loop Beta function for a general gauge group and anomalous dimensions beyond Feynman gauge. *JHEP* **10**, 166 (2017).
- [58] Chetyrkin, K. G., Falcioni, G., Herzog, F. & Vermaseren, J. A. M. Five-loop renormalisation of QCD in covariant gauges. *JHEP* **10**, 179 (2017). [Addendum: JHEP 12, 006 (2017)].
- [59] Harlander, R. V. & Neumann, T. The perturbative QCD gradient flow to three loops. *JHEP* **06**, 161 (2016).